ORGANOMETALLICS

Article

pubs.acs.org/Organometallics

Synthesis, Electronic Structure, and Reactivity of Palladium(I) Dimers with Bridging Allyl, Cyclopentadienyl, and Indenyl Ligands

Matthew J. Chalkley,[†] Louise M. Guard,[†] Nilay Hazari,*[,†] Peter Hofmann,[‡] Damian P. Hruszkewycz,[†] Timothy J. Schmeier,[†] and Michael K. Takase[†]

[†]The Department of Chemistry, Yale University, P.O. Box 208107, New Haven, Connecticut 06520, United States

[‡]Organisch-Chemisches Institut, University of Heidelberg, Im Neuenheimer Feld 270, D-69120 Heidelberg, Germany

Supporting Information

ABSTRACT: The synthesis of three new Pd(I) dimers, (μ-All)(μ-Cp){Pd(PEt_3)}$_2$ (All = C_3H_5, Cp = C_5H_5), (μ-All)(μ-Ind){Pd(PEt_3)}$_2$ (Ind = C_7H_9), and (μ-Cp)(μ-Ind){Pd(PEt_3)}$_2$, which contain a combination of bridging allyl, Cp, or indenyl ligands and are all supported by triethylphosphine as the ancillary ligand, is reported. The solid-state geometries, electronic structures, and reactivity of these new compounds have been compared with those of the dimers (μ-All)$_2${Pd(PEt_3)}$_2$ and (μ-Cp)$_2${Pd(PEt_3)}$_2$, which have previously been reported. This work establishes that there are many similarities in the solid-state and electronic structures of complexes containing bridging allyl, Cp, or indenyl ligands. For example, in all cases the bridging ligands bind through three carbon atoms to the two Pd atoms, with only the central carbon atom of the bridging group bound to both metal centers. However, there are also important differences based on the identity of the bridging ligand. As a result of different overlap between the metal centers and the π orbitals of the bridging allyl, Cp, or indenyl ligand, Cp ligands are more likely to result in an *anti* relationship between the two bridging ligands, while allyl and indenyl ligands are more likely to give a *syn* relationship. The solid-state structures indicate that bridging allyl ligands bind the most tightly to the metal center and bridging Cp ligands bind the least tightly. DFT calculations reveal that the nature of the bridging ligand alters the HOMO of the Pd(I) dimers. As a result, in some cases it is possible to selectively protonate one of the bridging ligands using the electrophile 2,6-lutidinium chloride.

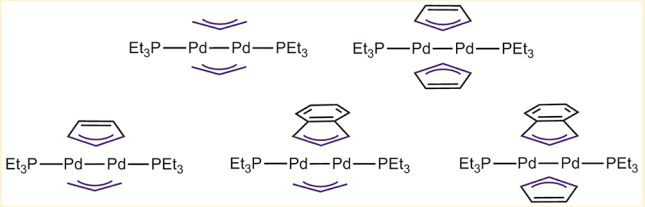

INTRODUCTION

Complexes containing Pd allyl moieties are crucial intermediates in a wide variety of important organic reactions,[1] such as allylic alkylation,[2] the telomerization of conjugated dienes,[3] and the electrophilic substitution of aldehydes, imines, and other Michael acceptors.[4] As a result, the chemistry of monomeric Pd(II) allyls is well understood, and it is accepted that η^1-allyls are nucleophilic and η^3-allyls are electrophilic.[1] In contrast, despite the synthesis of many Pd(I) dimers with bridging allyl ligands,[5] there have been relatively few studies of the reactivity of these systems and the electronic structure is not thoroughly understood. Preliminary work, performed mainly in the last 10 years, suggests that Pd(I) dimers containing bridging allyl ligands may play an important role as either catalysts or precatalysts in many organic transformations.[6] For example, in 2004, Milstein and co-workers used a Pd(I) dimer with one bridging allyl and one bridging chloride ligand as a precatalyst for the Suzuki–Miyaura coupling.[7] Subsequently, Moore et al. reported the use of related species for the Sonogashira coupling,[8] and Colacot and co-workers described that Pd(I) dimers were active precatalysts for the arylation of enolates and amines using aryl bromides and chlorides.[9] Recently our group described a family of unusual Pd(I) dimers with two bridging allyl ligands, which were catalysts for the carboxylation of allylstannanes and allylboranes using carbon dioxide.[10] Our mechanistic studies indicated that two bridging allyl ligands were essential for catalysis and species containing one bridging allyl ligand and one bridging chloride ligand were inactive.[10b]

In monomeric systems, the η^3-allyl ligand is often considered to be analogous to η^3-cyclopentadienyl (Cp) and η^3-indenyl ligands.[11] This analogy has been extended to dimeric Pd(I) complexes, and a number of systems containing bridging Cp or indenyl ligands, which are believed to be analogous to systems with two bridging allyl ligands[5d,10,12] (**AllAll**),[13] have been prepared. For example, Werner synthesized complexes containing one bridging allyl and one bridging Cp ligand[14] (**AllCp**) and two bridging Cp ligands[14a,15] (**CpCp**) with a range of terminal phosphines and phosphites, while complexes with two bridging indenyl ligands[16] (**IndInd**) have only been prepared with terminal isocyanides. However, to the best of our knowledge complexes containing one bridging allyl and one bridging indenyl ligand (**AllInd**) and one bridging Cp and one bridging indenyl ligand (**CpInd**) remain unknown. A summary of the different types of Pd(I) dimers that contain only bridging allyl, Cp, and indenyl ligands is shown in Figure 1.

At this stage preliminary spectroscopic, crystallographic, and theoretical evidence suggests that Pd(I) dimers with bridging

Received: May 11, 2013
Published: July 15, 2013

   dx.doi.org/10.1021/om400415c | *Organometallics* 2013, 32, 4223–4238

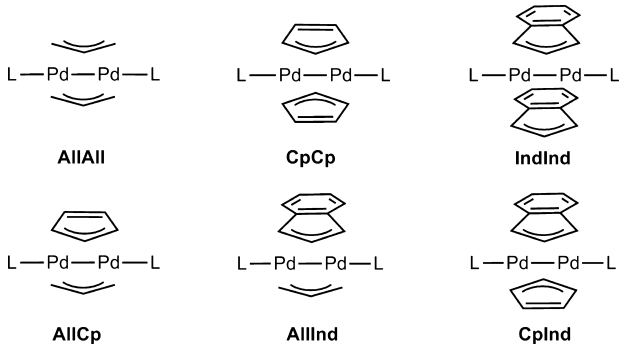

Figure 1. Generic pictures of bridging allyl dimers and related species. For references pertaining to **AllAll** systems see refs 5d, 10, and 12, for **CpCp** see refs 14a and 15, for **IndInd** see ref 16, and for **AllCp** see ref 14.

Cp or indenyl ligands are similar to species with bridging allyl ligands.[17] In the 1970s and 1980s, Werner and co-workers performed seminal work on the **AllCp** and **CpCp** systems, which demonstrated that in both cases the bridging Cp ligand was bound through three carbon atoms to the two Pd centers, in a fashion analogous to that for a bridging allyl ligand.[5a] This work was complemented by extended Hückel calculations by Hofmann, Hoffmann, and Dobosh on the bonding of Cp^- to a $(\mu\text{-Y})\{PdL\}_2^+$ (Y = Cl^-, SR^-, $COOR^-$, $C_3H_5^-$) fragment, which indicated that the bridging Cp ligand acted as a three-electron donor to the two Pd centers, consistent with the bridging Cp ligand being a surrogate for a bridging allyl ligand.[18] Related extended Hückel calculations by Yamamoto et al. on complexes with two bridging indenyl ligands (**IndInd**) supported by ancillary isocyanide ligands indicated that the bridging indenyl ligands also acted as three-electron donors to the two Pd centers.[16b] Although the reactivity of the **IndInd** systems has not been studied in detail, the **AllCp** and **CpCp** systems both displayed similar reactivities. The observed reactivity can be broken into two classes. In the first class, the binuclear core was retained, whereas in the second class two monomeric products were formed.[5a] Relatively soft electrophiles such as carboxylic acids and thiols were shown to retain the binuclear core, whereas reactions with other electrophiles such as HCl and MeI resulted in the cleavage of the binuclear core to form two monomeric products.[19]

One difficulty in comparing the structures and reactivity of species with bridging allyl, Cp, or indenyl moieties has been that the ancillary ligand has often been changed along with the bridging ligand. There are no examples of the preparation of a family of complexes supported by the same ancillary ligand. Given our observation that the presence of two bridging allyl ligands is crucial for catalytic carboxylation,[10a,b] we were interested in preparing all of the complexes shown in Figure 1, with the same ancillary ligand. Here, we perform the first complete comparison of bridging allyl, Cp, and indenyl ligands and also compare bridging Cp and indenyl ligands with η^3- and η^5-Cp and indenyl ligands bound to a single metal center. Specifically, we report the synthesis of three new Pd(I) dimers, **AllCp**, **AllInd**, and **CpInd**, supported by triethylphosphine ligands and compare their structure and reactivity with those of **AllAll** and **CpCp** with triethylphosphine ligands, which have previously been reported in the literature.[10a,15c] Unfortunately, attempts to prepare the **IndInd** dimer supported by triethylphosphine were unsuccessful.

RESULTS AND DISCUSSION

Synthesis. Given that the synthesis and X-ray structures of the complexes **AllAll** and **CpCp** supported by triethylphosphine ligands[10a,15c] had already been described in the literature, our aim was to prepare the new complexes **AllCp**, **AllInd**, **CpInd**, and **IndInd** supported by triethylphosphine ligands to complete the series shown in Figure 1.[20] The preparation of all of the allyl- and indenyl-containing dimers began from the two analogous air- and moisture-stable dinuclear Pd complexes $(\mu\text{-Cl})_2\{Pd(\eta^3\text{-allyl})\}_2$ ($\mathbf{I_{All2}}$)[21] and $(\mu\text{-Cl})_2\{Pd(\eta^3\text{-indenyl})\}_2$ ($\mathbf{I_{Ind2}}$), shown in Figure 2.[22] The preparation of $\mathbf{I_{Ind2}}$ was

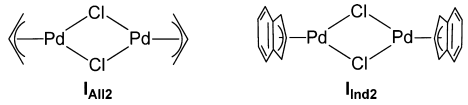

Figure 2. Analogous starting materials used for the synthesis of bridging allyl[21] and indenyl dimers.[22]

found to proceed most smoothly when the procedure described by Lin et al. was utilized,[22] whereas we were unable to synthesize $\mathbf{I_{Ind2}}$ using the route described by Murata et al.[23] as has been reported by others.[24]

*Synthesis of **AllCp**.* Previously, we have demonstrated that treatment of $\mathbf{I_{All2}}$ with allyl Grignard results in the formation of the literature complex $(\eta^3\text{-allyl})_2Pd$ ($\mathbf{II_{All2}}$),[21] which can be treated with triethylphosphine to generate **AllAll** in high yields.[10a] We postulated that it may be possible to form **AllCp** and **AllInd** through the treatment of the known complexes $(\eta^3\text{-allyl})(\eta^5\text{-Cp})Pd$ ($\mathbf{II_{AllCp}}$)[25] and $(\eta^3\text{-allyl})(\eta^5\text{-indenyl})Pd$ ($\mathbf{II_{AllInd}}$),[26] respectively, with triethylphosphine. $\mathbf{II_{AllCp}}$ was prepared in high yield from $\mathbf{I_{All2}}$ with NaCp. It is a thermally unstable complex but can be stored indefinitely at −30 °C in a glovebox. The addition of 1 equiv of triethylphosphine to $\mathbf{II_{AllCp}}$ resulted in the formation of **AllCp** at room temperature in good yield, 76% (Scheme 1). In this reaction, we propose that an equilibrium mixture of $(\eta^3\text{-allyl})(\eta^1\text{-Cp})Pd(PEt_3)$ and $(\eta^1\text{-allyl})(\eta^5\text{-Cp})Pd(PEt_3)$, which can be observed by ^1H NMR spectroscopy at low temperature, is initially formed. These highly reactive intermediates then reductively eliminate 5-allylcyclopenta-1,3-diene (or a related isomer) to give $Pd(PEt_3)$, which is trapped by another equivalent of $(\eta^3\text{-allyl})(\eta^1\text{-Cp})Pd(PEt_3)$ to give **AllCp**. Both our group and others have proposed an analogous mechanism for the formation of **AllAll** from $\mathbf{I_{All2}}$ and triethylphosphine,[10a,27] and Werner has previously characterized equilibrium mixtures related to $(\eta^3\text{-allyl})(\eta^1\text{-Cp})Pd(PEt_3)$ using low-temperature NMR spectroscopy.[28] In contrast to the case for **AllAll**,[10a] **AllCp** is unstable at room temperature in both solution and the solid state and slowly decomposes. However, it is stable indefinitely on storage in a glovebox at −30 °C.

*Synthesis of **AllInd**.* Attempts to use $(\eta^3\text{-allyl})(\eta^5\text{-indenyl})Pd$ ($\mathbf{II_{AllInd}}$) as a precursor for the formation of **AllInd** were unsuccessful. We believe that this is due to the thermal instability of $\mathbf{II_{AllInd}}$, which rapidly decomposed even at low temperature.[26] When $\mathbf{II_{AllInd}}$ was treated with triethylphosphine at low temperature, an inseparable mixture of **AllInd** and $Pd(PEt_3)_3$ was formed. Werner has previously encountered a similar problem in the synthesis of species containing one bridging allyl and one bridging Cp ligand.[14b] **AllInd** was prepared in good yield (68%) in two steps from **AllAll** (Scheme 2). We have previously shown that the treatment of

dx.doi.org/10.1021/om400415c | Organometallics 2013, 32, 4223−4238

Scheme 1

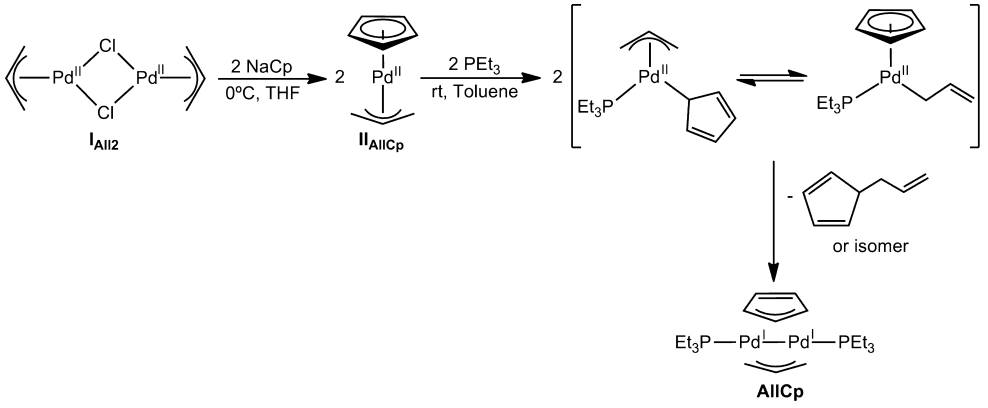

Scheme 2

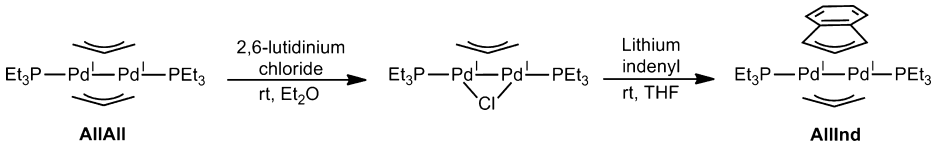

Scheme 3

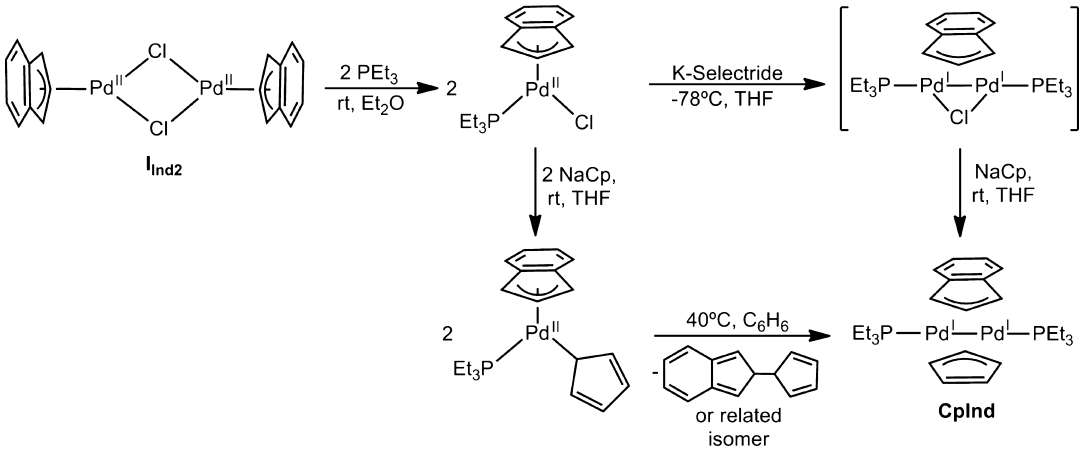

AllAll with anhydrous HCl in ether forms (μ-All)(μ-Cl){Pd(PEt$_3$)}$_2$, but a significant amount of Pd black is also generated.[10b] A more convenient route for the synthesis of (μ-All)(μ-Cl){Pd(PEt$_3$)}$_2$ is protonation of **AllAll** or **AllCp** with solid 2,6-lutidinium chloride, which is a stable HCl surrogate. Subsequent addition of lithium indenyl to (μ-All)(μ-Cl){Pd(PEt$_3$)}$_2$ results in the formation of **AllInd**. This is the first example of the synthesis of a complex containing one bridging allyl ligand and one bridging indenyl ligand. **AllInd** is thermally unstable in both solution and the solid state and decomposes over a period of several hours at room temperature.

Synthesis of ***CpInd****.* Two different routes could be used for the synthesis of **CpInd** (Scheme 3). In both cases the first step was the addition of triethylphosphine to $\mathbf{I_{Ind2}}$ to form (η^3-indenyl)PdCl(PEt$_3$), which was fully characterized. In the first route, this was followed by addition of NaCp to (η^3-indenyl)PdCl(PEt$_3$) to form the intermediate monomer (η^1-Cp)(η^3-indenyl)Pd(PEt$_3$), which was identified by the presence of a new resonance at 34.6 ppm in the ^{31}P{^{1}H} NMR spectrum and the growth of a Cp peak at 5.25 ppm in the ^{1}H NMR spectrum. This monomer could be converted to **CpInd** in 38% yield by heating for 12 h at 40 °C, presumably through reductive elimination of 2-(cyclopenta-2,4-dien-1-yl)-2*H*-indene or a related isomer. The elevated temperature and increased reaction time for this reaction in comparison to those for the syntheses of **AllAll** and **AllCp** suggest that the barrier for reductive elimination from (η^1-Cp)(η^3-indenyl)Pd(PEt$_3$) is higher than that for (η^1-allyl)(η^3-allyl)Pd(PEt$_3$) and (η^3-allyl)(η^1-Cp)Pd(PEt$_3$), which both readily form the dimers in minutes at room temperature. Werner has previously observed that conversion of (η^1-Cp)(η^3-Cp)Pd(PEt$_3$) to **CpCp** is also relatively difficult.[15c] The second route for the formation of **CpInd** involved the addition of 0.5 equiv of potassium tri-*sec*-butylborohydride (K-Selectride) to (η^3-indenyl)PdCl(PEt$_3$), followed by addition of 1 equiv of NaCp. It is proposed that this reaction proceeds via initial formation of (η^3-indenyl)-PdH(PEt$_3$), followed by reductive elimination of indene, to give Pd(PEt)$_3$, which is trapped by another equivalent of (η^3-indenyl)PdCl(PEt$_3$) to give (μ-Ind)(μ-Cl){Pd(PEt$_3$)}$_2$.[12b] In this case the in situ generated (μ-Ind)(μ-Cl){Pd(PEt$_3$)}$_2$ was

dx.doi.org/10.1021/om400415c | *Organometallics* 2013, 32, 4223−4238

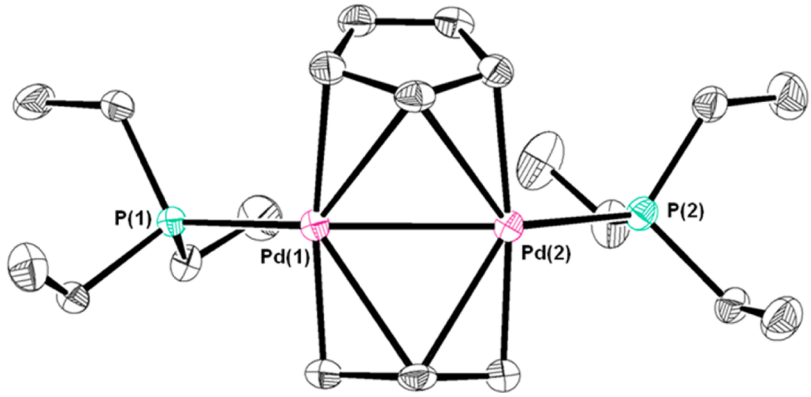

Figure 3. ORTEP[30] of **AllCp** with 30% probability ellipsoids. Hydrogen atoms are omitted for clarity.

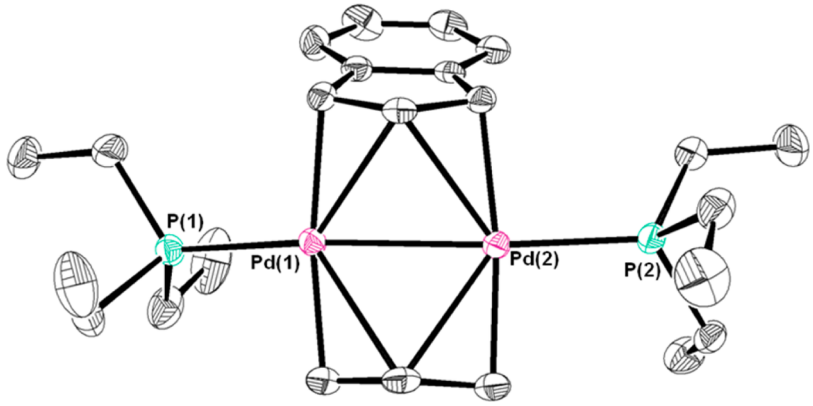

Figure 4. ORTEP[30] of **AllInd** with 30% probability ellipsoids. Hydrogen atoms are omitted for clarity.

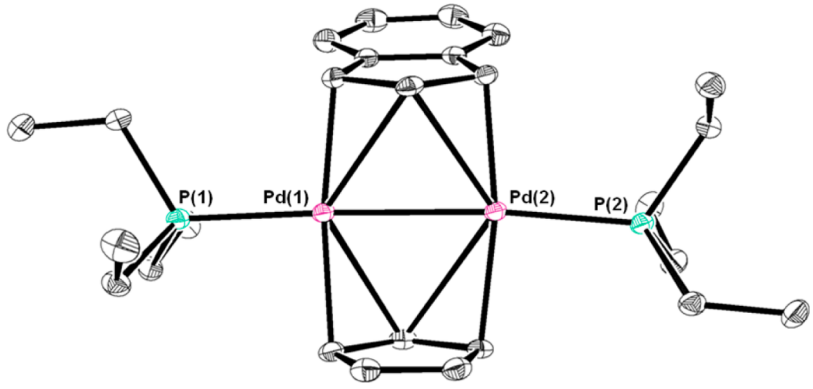

Figure 5. ORTEP[30] of **CpInd** with 30% probability ellipsoids. Hydrogen atoms are omitted for clarity.

Table 1. Comparison of Pd−Carbon and Pd−Pd Bond Lengths in AllAll,[a] AllCp, AllInd, CpCp, and CpInd

complex	bridging group	Pd(1)−$C_{terminal}$	Pd(2)−$C_{terminal}$	Pd(1)−$C_{central}$	Pd(2)−$C_{central}$	Pd−Pd
AllAll[a]	All	2.158(5)	2.106(5)	2.429(4)	2.611(4)	2.7112(4)
	All	2.120(5)	2.151(4)	2.613(4)	2.437(4)	
AllCp	All	2.082(5)	2.106(5)	2.524(4)	2.461(5)	2.6901(5)
	Cp	2.232(4)	2.219(4)	2.525(4)	2.568(5)	
AllInd	All	2.104(4)	2.089(4)	2.473(4)	2.515(4)	2.7098(5)
	Ind	2.171(4)	2.176(4)	2.521(4)	2.507(4)	
CpCp	Cp	2.168(2)	2.1745(19)	2.557(2)	2.546(2)	2.6865(5)
CpInd	Cp	2.186(3)	2.192(3)	2.669(3)	2.529(3)	2.6751(3)
	Ind	2.152(3)	2.134(3)	2.453(3)	2.488(3)	

[a]Data reported from ref 10a.

dx.doi.org/10.1021/om400415c | *Organometallics* 2013, 32, 4223−4238

not isolated or spectroscopically characterized but reacted directly with NaCp to give **CpInd** in 54% yield.

Attempted Synthesis of ***IndInd.*** A number of different routes were attempted for the synthesis of **IndInd**. These included treatment of the dimeric complex (μ-Ind)(μ-Cl)$\{$Pd(PEt$_3$)$\}_2$ with lithium indenyl at both low and room temperature and treatment of (η^3-indenyl)PdCl(PEt$_3$) with 1 equiv of lithium indenyl. In all cases at least two products were observed, and it was unclear by ^{1}H and ^{31}P NMR spectroscopy whether either of these products were **IndInd**. Repeated attempts to separate the mixture failed, as did attempts to grow single crystals from the mixture. It should be noted that Yamamoto and co-workers previously reported that their efforts to synthesize the triphenylphosphine analogue of **IndInd** were unsuccessful.[16b] Although it does not appear that there is an inherent reason why phosphine-supported versions of **IndInd** are unstable, to date these have remained elusive.

Solid-State Structures. As part of this work the solid-state structures of **AllCp**, **AllInd**, and **CpInd** were elucidated. These are shown in Figures 3−5, and a comparison of important bond lengths is shown in Table 1. Also included in Table 1 are the bond lengths from the solid-state structure of the previously reported **AllAll**.[10a] The structure of **CpCp** has also been previously reported,[15c] but during the course of this work we obtained a significantly higher quality structure and recorded diffraction data at low temperature. Although the old and new structures of **CpCp** are in different space groups, the bond lengths and angles are similar. Given the higher quality of the new structure, we have reported the data from that structure in Table 1 (see the Supporting Information for the new structure of **CpCp**). Table 2 provides information about the preferred geometry of the bridging ligands in the different complexes and the P−Pd−Pd bond angles.

Table 2. Experimental P−Pd−Pd Bond Angles and Preferred Orientation of the Bridging Ligands in AllAll,[a] AllCp, AllInd, CpCp, and CpInd

complex	P−Pd−Pd bond angle	bridging group orientation
AllAll[a]	157.47(4), 153.66(4)	*syn*
AllCp	152.52(3), 152.93(4)	*syn*
AllInd	171.56(3), 166.99(3)	*syn*
CpCp	175.714(16)	*anti*
CpInd	177.35(4), 174.65(2)	*anti*

[a]Data reported from ref 10a.

Analysis of the solid-state structures of the five compounds indicates that the bridging Cp and indenyl ligands bind in a similar fashion to the bridging allyl ligand. In the case of the bridging allyl ligand the central carbon is bound to both Pd centers, while the terminal carbons are bound to one Pd center each.[10a] This binding motif is reproduced in the case of the bridging Cp and indenyl ligands with a central carbon atom bound to both Pd centers and the adjacent carbon atoms bound to only one Pd center. There is clearly no interaction between the Pd centers and the olefinic carbons of the bridging Cp or the aromatic carbon atoms of the five-membered ring of the bridging indenyl ligand, as the Pd−C bond distances are almost 3 Å in all cases (Figure 6). Therefore, both the bridging Cp and indenyl ligands bind through only three carbon atoms to the two Pd centers. In this sense, the bridging Cp and indenyl ligands can be considered to be analogous to η^3-Cp and η^3-indenyl ligands in monomeric systems. The C−C bond distances in the bridging Cp and indenyl ligands are also consistent with those observed in monomeric η^3 systems, with two long bonds, two intermediate bonds, and one short bond observed for the bridging Cp ligand and two long bonds and three intermediate bonds observed for the five-membered ring of the bridging indenyl ligand.[29]

In general, Cp and indenyl ligands in monomeric η^3 systems are folded;[31] however, in our case the bridging Cp and indenyl ligands are planar. All of the fold angles are less than 10°,[32] which is typically indicative of η^5 binding of a Cp or indenyl ligand in monomeric systems.[33] The folding in monomeric systems is caused by one or two electrons populating an antibonding orbital between the metal and the Cp or indenyl ring.[34] Folding reduces the number of carbon atoms involved in the antibonding interaction from five to three, which greatly stabilizes the system but also reduces the strength of the metal−ligand bond.[34] In our bridging systems this antibonding orbital is not populated, as there are only 16 electrons around the metal centers; therefore, there is no need for the Cp or indenyl ring to fold. The underlying electronic reasons for why the bridging Cp or indenyl ligands binds as a three electron (LX type)[35] ligand are explored further in Computational Studies (vide infra). Analysis of other Pd(I) dimers in the literature with bridging Cp and indenyl ligands reveals that they have structural features similar to those described here.[12a,14−16,36] Furthermore, the binding of the bridging Cp or indenyl ligands in Pd systems is analogous to that described in other transition-metal systems with bridging Cp or indenyl ligands.[37] Overall, although it appears that bridging Cp and indenyl ligands bind in a similar fashion to bridging allyl ligands, they are structurally distinct from η^3- or η^5-Cp or indenyl ligands and require their own classification.

In all cases the bindings of the bridging ligand are not equivalent (Table 1). For example in **AllCp**, the Pd(1)−C bond distance to the terminal carbon of the bridging allyl ligand is 2.082(5) Å, while the Pd(2)−C bond distance to the other terminal carbon of the bridging allyl ligand is 2.106(5) Å. The bindings of the Pd centers to the central carbon of the bridging ligand are also inequivalent. In **AllCp**, the Pd(1)−C bond distance to the central carbon of the bridging allyl ligand is 2.524(4) Å and the Pd(2)−C bond distance is 2.461(5) Å. This

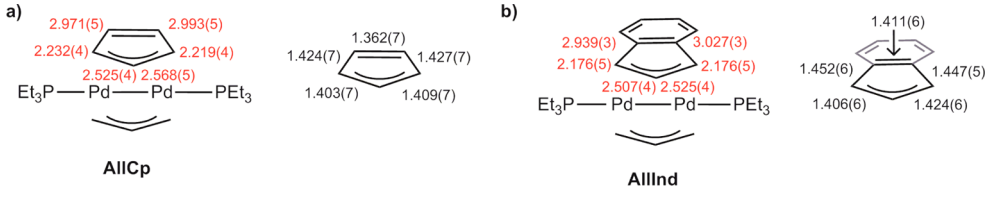

Figure 6. Selected bond lengths and distances involving (a) the bridging Cp ligand of **AllCp** and (b) the bridging indenyl ligand in **AllInd**. C−C bond distances are shown in black, and Pd−C bond distances are in red. All distances are in Å.

dx.doi.org/10.1021/om400415c | *Organometallics* 2013, 32, 4223−4238

effect is most pronounced for **AllAll**, where there is a difference of approximately 0.18 Å between the Pd−C bond distances to the central carbon of the bridging allyl ligand. The binding of the second bridging ligand is complementary to the first. Thus, because in **AllCp** the Pd(1)−C distance to the terminal carbon of the bridging allyl ligand is shorter than the corresponding Pd(2)−C bond distance to the other terminal carbon of the bridging allyl ligand; the opposite is observed when considering the binding of the Cp ligand. For the bridging Cp ligand in **AllCp**, the Pd(2)−C bond distance to the terminal carbon of the Cp ligand is 2.219(4) Å, while the corresponding Pd(1)−C bond distance to the other terminal carbon is longer at 2.232(4) Å. The same effect is also present when considering the binding to the central carbon atom of the bridging ligand.

A comparison of the respective bond lengths from the Pd centers to both the terminal carbons and the central carbons of the bridging ligands in **AllCp**, **AllInd**, and **CpInd** indicates that the Pd−bridging allyl bond distances are the shortest, followed by the Pd−bridging indenyl and Pd−bridging Cp bond distances. This suggests that the bridging allyl binds the most tightly, followed by the bridging indenyl ligand and then the bridging Cp ligand (Table 1). Additional support for this hypothesis is provided by the elongation of the bond lengths in mixed systems with a more tightly bound fragment in comparison to the species which have two of the same bridged species. For example, in **CpCp**, the average Pd−C terminal distance is 2.17 Å, whereas in **AllCp** the average Pd−C terminal distance of the bridging Cp ligand is 2.22 Å. This indicates that the bridging allyl ligand has a greater *trans* influence than the bridging Cp ligand, consistent with tighter binding of the bridging allyl ligand. Finally, the length of the Pd−Pd bond contracts with more weakly bound bridging fragments, with the shortest bond lengths being observed in **CpInd** (2.6751(3) Å) and **CpCp** (2.6865(5) Å) and the longest bond length in **AllAll** (2.7112(4) Å).

One of the most striking features of the family of complexes is the difference in the orientation of the bridging ligands (Table 2). In **AllAll**, **AllCp**, and **AllInd** the two bridging ligands are oriented in a *syn* geometry, so that the central carbon atoms of the bridging ligands are eclipsed and are located on the same face of the molecule. In contrast, in **CpCp** and **CpInd** the two bridging ligands are oriented in an *anti* configuration, so that the central carbon atoms are on opposite faces of the molecules. The electronic reasons for this difference are described as part of our computational studies (vide infra). Some of the major differences between the *syn* and *anti* geometries are the P−Pd−Pd bond angles. In the *anti* structures this angle is close to 180°, whereas in the *syn* structures it is significantly less than 180° and ranges from 150 to 170°. In all *syn* structures the triethylphosphine ligands are bent away from the central carbon atom of the bridging ligands. In the case of **AllInd**, the P−Pd−Pd bond angle is closer to linear than in the other *syn* systems, presumably to minimize an unfavorable steric interaction between protons on the ethyl group of the triethylphosphine ligand and the aromatic protons on the indenyl ring. In the *anti* configuration, bending the P−Pd−Pd bond angle will decrease the steric clash between the triethylphosphine ligand and one of the bridging groups but increase the steric clash with the other bridging group. As a result, almost no bending occurs.

Previously, we have noted that, in complexes containing two bridging allyl ligands, the central carbon atom of the bridging allyl ligand is canted toward the Pd centers. As a result, the dihedral angle between the bridging allyl plane and the plane containing the two Pd atoms and the two terminal carbon atoms of the bridging allyl ligand (the dihedral angle θ in the diagram accompanying Table 3) is significantly less than 90°.[10b]

Table 3. Calculated Values of the Dihedral Angle Formed Between the Allyl, Cp, or Indenyl Plane and the Plane Containing the Two Pd Centers and the Two Terminal Carbon Atoms of the Bridging Allyl, Cp, or Indenyl Ligand in AllAll,[a] AllCp, AllInd, CpCp,[b] and CpInd

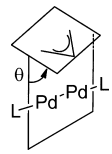

compd	θ (deg)
AllAll[a]	81.1, 81.3
AllCp	81.6 (All), 75.5 (Cp)
AllInd	81.7 (All), 76.1 (Ind)
CpCp	79.5, 79.5
CpInd	82.6 (Cp), 74.8 (Ind)

[a]Data reported from ref 10a.

We proposed that this was due to a back-bonding interaction from the Pd−Pd bond to the LUMO of the allyl ligand. Kurosawa et al. reported a similar result for species with one bridging allyl ligand and one bridging halide ligand.[38] The values of this dihedral angle are summarized for the full family of complexes in Table 3. A similar canting toward the metal is observed for both bridging Cp and indenyl ligands, which suggests that these ligands are also able to accept back-donation from the Pd centers. This stands in contrast to η^3-Cp or η^3-indenyl ligands and metal centers, where the central carbon of the ligand is almost always canted away from the metal center.[39] From our data it appears that the extent of distortion is greatest for indenyl and smallest for allyl.

NMR Analysis. The use of ^{1}H and ^{13}C NMR spectroscopy to determine the hapticity of monomeric allyl, Cp, and indenyl systems is common.[40] In this case, the ^{1}H and ^{13}C NMR spectra of the allyl fragment in all complexes which contain a bridging allyl ligand are similar to those reported for symmetrical monomeric η^3-allyls.[41] In the ^{1}H NMR spectrum, the central allyl proton always appears as a complex multiplet, while the terminal *syn* CH_2 protons appear as a quartet and the terminal *anti* CH_2 protons appear as a doublet. The *syn* protons are those that are on the same side of the allyl fragment as the central proton, while the *anti* protons are those on the opposite side of the allyl fragment. In the ^{13}C NMR spectrum only two resonances are observed for the bridging allyl ligand. Interestingly, the ^{1}H NMR chemical shifts for the central proton and the terminal *anti* CH_2 protons of the bridging allyl ligand decrease as the donor power of the other bridging ligand decreases (Table 4). For example, in **AllInd**, the ^{1}H NMR chemical shift for the central proton of the bridging allyl ligand is 3.79 ppm, while the corresponding proton resonates at 3.00 ppm in **AllCp**, which contains the much more weakly donating Cp ligand opposite the allyl ligand. The same trend is also observed for the central carbon resonances of the bridging allyl ligand in the ^{13}C NMR spectra of **AllAll**, **AllInd**, and **AllCp**. In contrast, there is no trend in the ^{1}H NMR chemical shifts of the terminal *syn* CH_2 protons of the allyl ligands or the ^{13}C NMR

dx.doi.org/10.1021/om400415c | *Organometallics* 2013, 32, 4223−4238

Table 4. ^{1}H and ^{13}C NMR Chemical Shifts for the Bridging Allyl Ligand in AllAll, AllInd, and AllCp and ^{31}P NMR Chemical Shifts for the Ancillary Triethylphosphine Ligand[a]

	^{1}H NMR			^{13}C NMR		
compd	$H_{central}$	H_{anti}	H_{syn}	$C_{central}$	$C_{terminal}$	^{31}P NMR PEt_3
AllAll[b]	3.86	1.77	2.72	86.70	27.80	14.2
AllInd	3.79	1.10	2.79	78.67	28.30	10.8
AllCp	3.00	0.99	2.72	74.32	25.59	9.1

[a]All chemical shifts are reported in ppm. [b]Data reported from ref 10a.

shifts of the terminal carbon atoms of the allyl ligand. A clear pattern is also present in the ^{31}P NMR chemical shifts. In the species with the most tightly bound bridging ligands the ^{31}P NMR chemical shift is greater than in those with more weakly bound bridging ligands. Thus, the ^{31}P NMR chemical shift for **AllAll**, which contains two highly donating bridging allyl ligands, is 14.2 ppm, while the ^{31}P NMR chemical shift for **AllCp**, which contains a more weakly donating bridging Cp ligand, is 9.1 ppm. This trend in the ^{31}P NMR chemical shifts is general for all compounds studied in this work.

For all dimers containing a bridging Cp ligand, a single resonance was observed for the Cp ligand in both the ^{1}H and ^{13}C NMR spectra at room temperature (Table 5). Even at

Table 5. ^{1}H and ^{13}C NMR Chemical Shifts for the Bridging Cp Ligand in AllCp, CpInd, and CpCp and and ^{31}P NMR Chemical Shifts for the Ancillary Triethylphosphine Ligand[a]

compd	^{1}H NMR Cp	^{13}C NMR Cp	^{31}P NMR PEt_3
AllCp	6.05	88.24	9.1
CpInd	5.64	88.04	5.2
CpCp[b]	5.60	87.75	4.1

[a]All chemical shifts are reported in ppm. [b]Data reported from ref 18 but independently verified in this study.

temperatures as low as −90 °C, only one resonance was present for the bridging Cp ligand in the ^{1}H NMR spectrum, which suggests that rotation of the bridging Cp ligand is facile. Werner has previously described similar NMR behavior of species containing bridging Cp ligands.[5a] In all cases, the single resonance in the ^{1}H NMR spectrum was a triplet due to coupling of around 2 Hz from the triethylphosphine ligands. The ^{1}H NMR shifts fall within the standard range for monomeric η^1-Cp complexes, which generally resonate between 5.6 and 6.0 ppm.[40a] In contrast, the ^{13}C NMR shifts fall within the standard range, 70−93 ppm, for monomeric η^5-Cp complexes.[40a] Although the sample size for conclusions based on our NMR data is small, this again suggests that the bridging Cp ligand needs to be considered differently from η^1-, η^3-, and η^5-Cp ligands. In a fashion analogous to that for bridging allyl ligands, the ^{1}H and ^{13}C NMR chemical shifts for the bridging Cp ligands decrease as the donor power of the other bridging ligand decreases.

In monomeric systems containing indenyl ligands it is easy to identify an η^1-indenyl ligand but significantly more difficult to differentiate between η^3- and η^5-indenyl ligands on the basis of ^{1}H NMR spectrscopy.[40c] In the ^{1}H NMR spectra of **CpInd** and **AllInd**, the central indenyl peaks appear as pentets generated by two overlapping triplets between 3.9 and 4.8 ppm, while the terminally bound indenyl peaks appear as doublets of triplets between 5.5 and 6.5 ppm (Table 6). Phosphorus decoupling simplifies these peaks into a triplet and a doublet, respectively.

Table 6. ^{1}H and ^{13}C NMR Chemical Shifts for the Bridging Indenyl Ligands in AllInd and CpInd[a]

	^{1}H NMR		^{13}C NMR		
compd	$H_{central}$	$H_{terminal}$	$C_{central}$	$C_{terminal}$	$\Delta\delta(^{13}C)$
AllInd	4.76	6.04	91.37	49.08	16
CpInd	3.92	5.74	88.04	47.78	18

[a]All chemical shifts are reported in ppm. $\Delta\delta(^{13}C)$ = the ^{13}C NMR chemical shift of the ring junction carbons in the complex minus the ^{13}C NMR chemical shift of the ring junction carbons in sodium indenide.

The protons associated with the six-membered ring of the indenyl ligands are complex multiplets between 7.0 and 8.0 ppm. Overall, the observed ^{1}H NMR chemical shifts and peak pattern for the bridging indenyl ligands are similar to those observed in monomeric complexes containing either η^3- or η^5-indenyl ligands.[42] Typically, ^{13}C NMR spectroscopy has been used to differentiate between η^3 and η^5 coordination of indenyl ligands in monomeric systems.[40b,c] Comparison of the ^{13}C NMR shift of the ring junction carbons with that found in sodium indenide, as defined in Table 6, has been well established as a quantitative measure of the hapticity of indenyl complexes.[40b,c] Baker and Tulip demonstrated that $\Delta\delta(^{13}C)$ values between −40 and −20 ppm were consistent with planar η^5-indenyls, values between −20 and −10 ppm corresponded to distorted η^5-indenyls, and values between +5 and +30 ppm were consistent with η^3-indenyls.[43] In the case of our complexes with bridging indenyl ligands the $\Delta\delta(^{13}C)$ values are similar to those observed for η^3-indenyl coordination in monomeric systems, although the significance of this observation is unclear. For the two complexes with bridging indenyl ligands, there is also a reduction in the ^{1}H and ^{13}C NMR chemical shifts when a more weakly bound fragment is opposite the bridging indenyl.

Computational Studies. DFT studies were performed in order to compare the electronic structures of our family of complexes. For the sake of comparison, **IndInd**, which we were unable to make, was also included. All calculations were performed using the trimethylphosphine ligand instead of the triethylphosphine ligand for computational simplicity. The calculated complexes have a prime after the compound name (for example **AllAll′**) to indicate that a trimethylphosphine ancillary ligand was used. Initially, the structure of a Pd(I) dimer with two bridging allyl ligands and two ancillary trimethylphosphine ligands (**AllAll′**) was optimized using a variety of different functionals (see Figure 7 and the Supporting Information for details). Computationally, the well-known functionals B3LYP, BMK, and M062X were unable to model the inequivalent binding of the bridging allyl ligand (vide supra) and predicted symmetrical binding of the allyl ligand to the Pd centers: i.e., that the Pd(1)−C bond distance to the terminal carbon atom of the bridging allyl ligand was identical with the Pd(2)−C bond distance to the other terminal carbon atom of the bridging allyl ligand. However, a variety of other pure and hybrid functionals, including BP86, BVP86, BPBE, BPW91, PBE, and TPSSH, were able to reproduce the inequivalent binding of the bridging allyl to the Pd atoms (see the Supporting Information). Most of these functionals produced a structure more accurate than that obtained from an MP2 calculation, which greatly overestimated the inequivalent binding of the bridging allyl ligand to the Pd centers. The hybrid functional TPSSH was able to reproduce the

dx.doi.org/10.1021/om400415c | Organometallics 2013, 32, 4223−4238

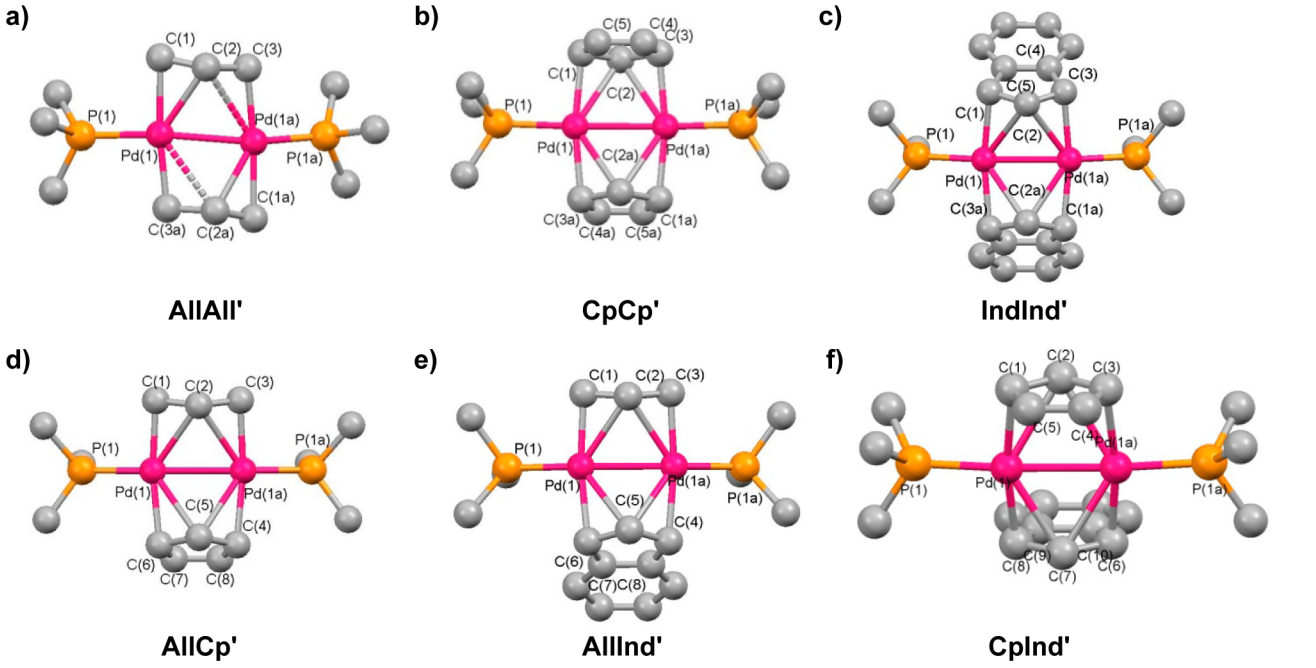

Figure 7. Optimized structures of (a) **AllAll′**, (b) **CpCp′**, (c) **IndInd′**, (d) **AllCp′**, (e) **AllInd′**, and (f) **CpInd′**. Hydrogen atoms have been omitted from all structures for clarity.

experimental bond lengths and distances the most accurately and was utilized for all further analysis.

The structures of **AllCp′**, **AllInd′**, **CpCp′**, **CpInd′**, and **IndInd′** were all optimized using the TPSSH functional (Figure 7 and Table 7). In general, excellent agreement was observed between calculated and experimental bond lengths and angles (see the Supporting Information). One of the defining geometrical features of the compounds bridged by Cp or indenyl ligands is that only three carbons are involved in the bonding to Pd and our models were able to correctly predict this binding mode. The X-ray structure of **CpCp** shows that the bindings of the bridging Cp ligands to the Pd centers are not equivalent. As a result, the Pd(1)−C(1) bond distance is not the same as the Pd(1a)−C(3) bond distance, in a fashion analogous to the binding of the bridging allyl ligand, although the magnitude is considerably smaller. Unfortunately, in the case of the model compound **CpCp′**, we were unable to predict the inequivalent binding; however, given that our models were able to reproduce all other major structural features, we do not believe this is a major problem.

One notable difference between the lowest energy structures of our family of complexes is that in some cases the *syn* isomer is preferred, while in other cases the *anti* isomer is the most stable. The relative energies of the *syn* and *anti* isomers of the different complexes are given in Table 8. Consistent with experimental results, the *anti* isomer is preferred for **CpCp′** and **CpInd′**, while the *syn* isomer is favorable for all other compounds. In some cases, the energy difference between the *syn* and *anti* isomers is quite small; however, even at low temperatures we have not been able to see two isomers by ^{1}H NMR spectroscopy. One possible explanation for our inability to see two isomers is that even at low temperature the isomers are in rapid exchange and only an averaged signal is observed.

Fragment Analysis of Bonding in the Bis(allyl) Complex AllAll′. In order to understand the electronic structure of **AllAll′**, a molecular orbital analysis was performed using the fragment approach pioneered by Hoffmann.[44] The fragments chosen were an allyl (C_3H_5) fragment and a (μ-C_3H_5)\{$Pd_2(PMe_3)$\}$_2$ fragment (this fragment is further broken down in the Supporting Information). The fragment orbital interaction diagram is shown in Figure 8, with selected isosurfaces for the molecular orbitals of **AllAll′** shown in Figure 9. There are four orbitals at low energy in the molecular orbital diagram of **AllAll′**, HOMO-11 to HOMO-14 (orbitals 97−100), which consist of linear combinations of the Pd−PMe_3 σ-bonding orbitals and the two π_1 orbitals of the allyl ligands. There is no significant interaction between the allyl ligand and the Pd centers in these orbitals. The most important bonding interaction between the (μ-C_3H_5)\{$Pd(PMe_3)$\}$_2$ fragment and the C_3H_5 fragment occurs in the HOMO-10 (orbital 101) and uses the π_2 orbital of the allyl fragment. Molecular orbital 101 is formed from orbital 90 of the (μ-C_3H_5)\{$Pd(PMe_3)$\}$_2$ fragment, which itself consists of a bonding interaction between the π_2 orbital of the allyl ligand and one of the antibonding Pd−Pd δ* orbitals of the Me_3P−Pd−Pd−PMe_3 fragment. Thus, the predominant interaction between the Pd centers and both bridging allyl ligands occurs through the π_2 orbital of the allyl ligand, in a fashion similar to that for the binding of η^3-allyls to monomeric Pd centers.[11]

There are nine orbitals, HOMO-9 to HOMO-1 (orbitals 102−110), in **AllAll′** that are predominantly centered on the two Pd atoms, which is consistent with two Pd(I) centers with a metal−metal single bond. The allyl ligands partially contribute to two of these orbitals. The HOMO-8 (orbital 103) contains two Pd centers that are weakly π bonding to each other and have a small amount of overlap with the π_1 orbitals of both of the allyl ligands. More importantly, the HOMO-2 (orbital 109) contains almost 15% combined contribution from the π_3 orbitals of the allyl ligands, consistent with significant back-donation from the Pd to the bridging allyl ligands. Kurosawa and co-workers have previously postulated that this back-donation causes the central carbon in complexes of the type (μ-C_3H_5)(μ-Br)\{$Pd(PH_3)$\}$_2$ to cant toward the metal centers,[38,43] and our results are consistent with this explanation.

dx.doi.org/10.1021/om400415c | *Organometallics* 2013, 32, 4223−4238

Table 7. Selected Bond Lengths and Angles from the Optimized Structures of AllAll′, CpCp′, IndInd′, AllCp′, AllInd′, and CpInd′[a]

bond length or angle	AllAll′	CpCp′	IndInd′	AllCp′	AllInd′	CpInd′
Pd(1)−Pd(1a)	2.75	2.70	2.71	2.73	2.74	2.70
Pd(1)−C(1)	2.21	2.21	2.20	2.14	2.14	2.22
Pd(1)−C(2)	2.42	2.60	2.53	2.54	2.55	2.63
Pd(1a)−C(3)	2.14	2.21	2.20	2.14	2.14	2.22
Pd(1a)−C(2)	2.75	2.60	2.53	2.54	2.55	2.63
Pd(1a)−C(1a)	2.22	2.20	2.20	–	–	–
Pd(1a)−C(2a)	2.42	2.57	2.53	–	–	–
Pd(1)−C(2a)	2.75	2.57	2.53	–	–	–
Pd(1)−C(3a)	2.15	2.20	2.20	–	–	–
Pd(1a)−C(4)	–	–	–	2.24	2.22	–
Pd(1a)−C(5)	–	–	–	2.58	2.54	–
Pd(1)−C(5)	–	–	–	2.58	2.54	–
Pd(1)−C(6)	–	–	–	2.24	2.22	–
Pd(1a)−C(6)	–	–	–	–	–	2.17
Pd(1a)−C(7)	–	–	–	–	–	2.53
Pd(1)−C(7)	–	–	–	–	–	2.53
Pd(1)−C(8)	–	–	–	–	–	2.17
C(1)−C(2)	1.41	1.43	1.44	1.43	1.43	1.43
C(1)−C(5)	–	1.46	1.47	–	–	1.46
C(2)−C(3)	1.45	1.43	1.44	1.43	1.43	1.43
C(3)−C(4)	–	1.46	1.47	–	–	1.46
C(4)−C(5)	–	1.38	1.43	1.44	1.44	1.38
C(4)−C(8)	–	–	–	1.45	1.47	–
C(5)−C(6)	–	–	–	1.44	1.44	–
C(6)−C(7)	–	–	–	1.45	1.47	1.44
C(6)−C(10)	–	–	–	–	–	1.47
C(7)−C(8)	–	–	–	1.38	1.43	1.44
C(8)−C(9)	–	–	–	–	–	1.47
C(9)−C(10)	–	–	–	–	–	1.43
P(1)−Pd(1)−Pd(1a)	161.2	177.0	157.5	156.4	156.3	176.6
P(1a)−Pd(1a)−Pd(1)	161.0	177.0	157.5	156.4	156.4	176.6

[a]All bond lengths are in Å, and all bond angles are in deg.

Table 8. Relative Energies ($\Delta G°$) of *syn* and *anti* Isomers of Families of Complexes[a]

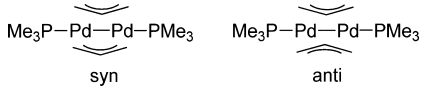

syn anti

compd	*syn*	*anti*
AllAll′	0	12.4
AllCp′	0	11.0
AllInd′	0	13.6
IndInd′	0	4.8
CpCp′	4.2	0
CpInd′	2.6	0

[a]Relative energies are given in kJ mol^{-1} with the lowest energy structure assigned as being at 0 kJ mol^{-1}.

As we have previously noted, the HOMO of **AllAll′** is almost entirely ligand based and is comprised of the out-of-phase combination of the two π_2 orbitals of the bridging allyl ligands.[10b] The symmetry of this out-of-phase combination of two π_2 orbitals permits interaction with only the Pd 5p orbitals, which are high in energy and unable to have a significant interaction with the allyl ligands. The HOMO−LUMO gap in **AllAll′** is quite large (3.8 eV), consistent with the compounds being pale yellow or colorless. The LUMO is metal−ligand antibonding with respect to both the allyl and trimethylphosphine ligands, which presumably explains why it is raised so high in energy.

Overall the bonding in **AllAll′** shares some similarities to that described by Kurosawa for $(\mu\text{-}C_3H_5)(\mu\text{-}Br)\{Pd(PH_3)\}_2$.[38] However, as described previously, the HOMO of **AllAll′** is localized on the ligand orbitals, whereas that of $(\mu\text{-}C_3H_5)(\mu\text{-}Br)\{Pd_2(PH_3)\}_2$ and the related species $(\mu\text{-}C_3H_5)(\mu\text{-}Cl)\{Pd(PMe_3)\}_2$ is mainly centered on the metal and only includes a small ligand contribution (from back-bonding between the metal and the π_3 orbital of the allyl ligand).[10b,38] As a result we suggest that the bridging allyl ligands in **AllAll′** are significantly more likely to react with electrophiles than the single bridging allyl ligand in the chloride- and bromide-bridged species.

Comparison of Bonding in AllAll′ with That in AllCp′ and AllInd′. Using the same fragment approach described above, the bonding in **AllAll′** can be easily compared to the bonding in **AllCp′** and **AllInd′**. In these cases a Cp or indenyl fragment is added to a $(\mu\text{-}C_3H_5)\{Pd(PMe_3)\}_2$ fragment. The Cp fragment has five frontier orbitals formed from linear combinations of the carbon 2p orbitals (Figure 10a). The lowest energy of these orbitals is the completely in-phase bonding combination (π_{1Cp}), which does not interact in any significant fashion with the metal orbitals of the $(\mu\text{-}C_3H_5)\{Pd(PMe_3)\}_2$ fragment. This is followed by two orbitals (π_{2aCp} and π_{2bCp}), which contain one node between the carbon 2p orbitals. The most significant interaction between the Cp fragment and the $(\mu\text{-}C_3H_5)\{Pd(PMe_3)\}_2$ fragment involves the π_{2bCp} orbital. This orbital interacts with the $(\mu\text{-}C_3H_5)\{Pd(PMe_3)\}_2$ fragment in the same way as the π_2 orbital (12) of the allyl fragment in **AllAll′** (see Figure 8). The in-phase combination of the π_{2bCp} orbital and the π_2 orbital of the bridging allyl ligand of the $(\mu\text{-}C_3H_5)\{Pd(PMe_3)\}_2$ fragment forms a low-energy bonding orbital (HOMO-11 in Figure 10b), while the out-of-phase combination is not of the correct symmetry to easily overlap with the metal orbitals and forms a high-energy orbital (HOMO-1). However, whereas in **AllAll′** there is no metal contribution to the out-of-phase combination of the two π_2 orbitals of the allyl ligands, there is a small amount of metal character in this case. In contrast to the case for π_{2bCp}, π_{2aCp} is not of the correct symmetry to interact with the metal 4d orbitals and remains nonbonding. The HOMO of **AllCp′** is largely comprised of the π_{2aCp} orbital, which is consistent with the Cp ligand formally acting as a three-electron donor. It also suggests that electrophiles may preferentially react at the bridging Cp ligand rather than the bridging allyl ligand. Between the HOMO-11 and HOMO-1, there are nine orbitals which are predominantly linear combinations of the metal 4d orbitals. In an analogous fashion to **AllAll′**, one of these orbitals (HOMO-3) contains a small back-bonding interaction between one of the unfilled Cp orbitals (π_{3aCp}) and the metal center.

The electronic structure of the bridging indenyl complex **AllInd′** is similar to that of the bridging Cp complex **AllCp′**. The frontier orbitals of the indenyl fragment are slightly more complicated than those of the Cp fragment because of both in-phase and out-of-phase contributions from the π system of the phenyl ring to the Cp-like indenyl orbitals. However, there are six key orbitals that need to be considered (Figure 11a). These orbitals are related to those described for the Cp fragment. The lowest energy frontier orbital of the indenyl fragment, π_{1In}, does not interact with any metal orbitals, while the predominant

dx.doi.org/10.1021/om400415c | Organometallics 2013, 32, 4223−4238

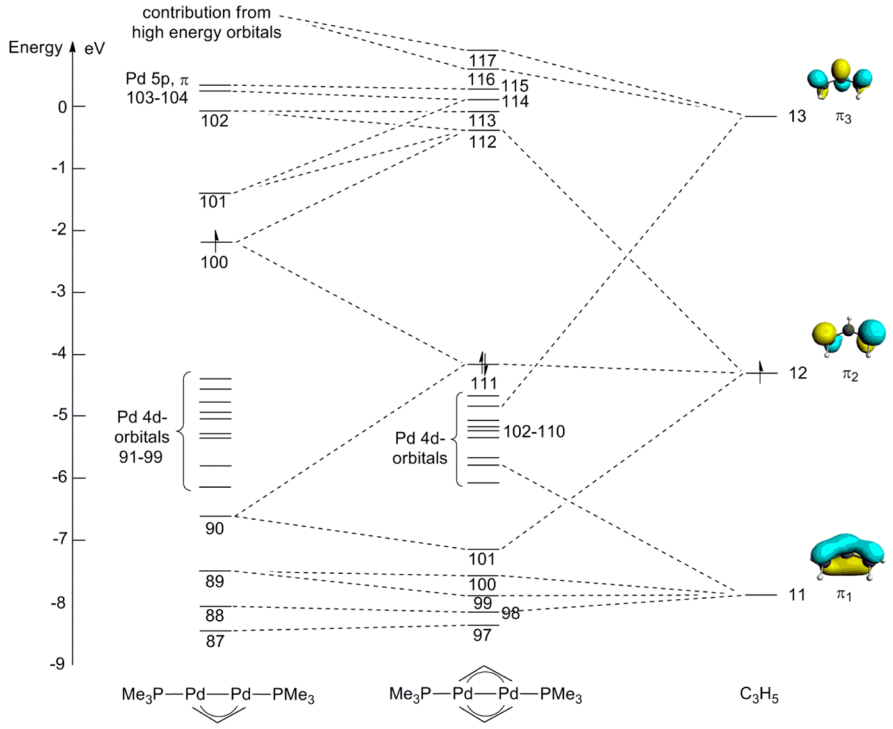

Figure 8. Fragment orbital interaction diagram for **AllAll′** constructed from neutral $(\mu\text{-}C_3H_5)\{Pd(PMe_3)\}_2$ and C_3H_5 fragments.

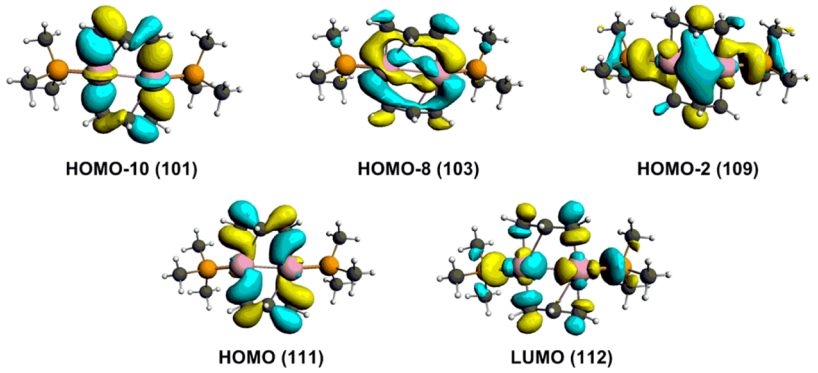

Figure 9. Selected molecular orbitals of **AllAll′**.

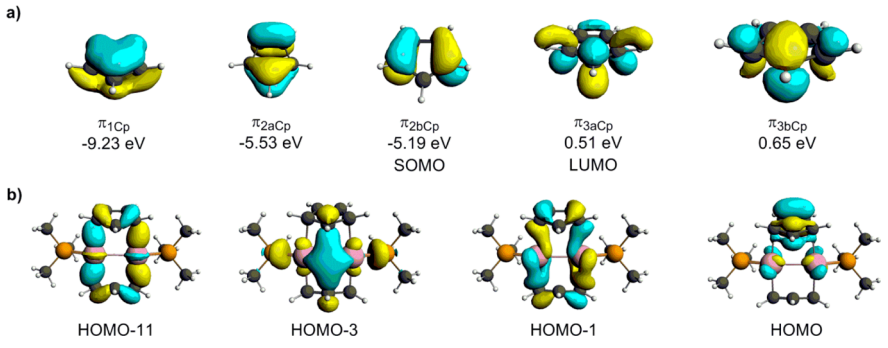

Figure 10. (a) Frontier molecular orbitals of the Cp fragment. (b) Selected molecular orbitals of **AllCp′**.

interaction between the metal and indenyl fragment occurs using the $\pi_{2bIn(1)}$ and the $\pi_{2bIn(2)}$ orbitals. These orbitals are related to the π_{2bCp} orbital of the Cp ligand (vide supra), with $\pi_{2bIn(1)}$ being in phase with the phenyl ring π system, while $\pi_{2bIn(2)}$ is out of phase. A linear combination of the $\pi_{2bIn(1)}$ and the $\pi_{2bIn(2)}$ orbitals which is in phase with the π_2 orbital of the bridging allyl forms a strongly bonding orbital (HOMO-12 in Figure 11b). The out-of-phase combination of the π_2 orbital of the bridging allyl and the $\pi_{2bIn(1)}$ orbital of the indenyl fragment forms a low-energy orbital (HOMO-9) with the metal center stabilizing the π_2 orbital of the bridging allyl, while the out-of-phase combination of the π_2 orbital of the bridging allyl and the

dx.doi.org/10.1021/om400415c | *Organometallics* 2013, 32, 4223−4238

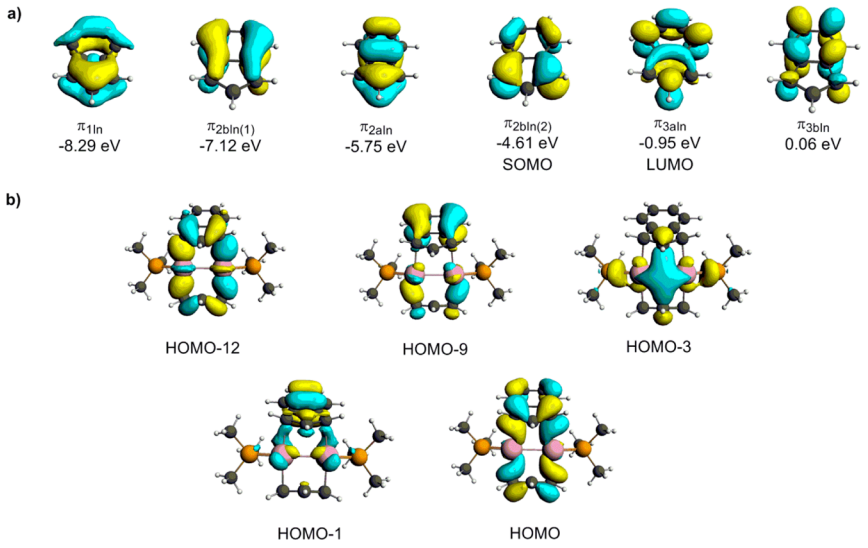

Figure 11. (a) Frontier molecular orbitals of the indenyl fragment. (b) Selected molecular orbitals of **AllInd′**.

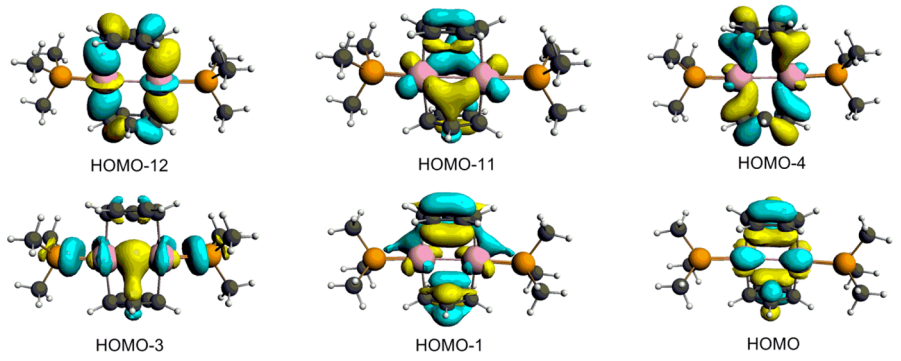

Figure 12. Selected molecular orbitals of **CpCp′**.

$\pi_{2bln(2)}$ of the indenyl fragment form a high-energy orbital (HOMO). There is no significant metal contribution to this out-of-phase combination, and as a result of the lack of stabilization from the metal, this orbital is raised in energy in comparison to the nonbonding indenyl orbital π_{2aln}, which is the HOMO-1. This is an ordering opposite to that described for **AllCp′**, and both the bridging indenyl and allyl ligands appear to be equally likely to undergo electrophilic attack in **AllInd′**. In fact, the nature of the HOMO in **AllInd′** is identical with that described for **AllAll′**. The HOMO-3 of **AllInd′** indicates that there is back-donation from the metal to the indenyl fragment in a fashion analogous to the back-donation described for complexes **AllAll′** and **AllCp′**.

Bonding in the Sandwich Compounds CpCp′ and IndInd′. The electronic structure of the bis(indenyl) complex **IndInd′** (see the Supporting Information) is similar to that of **AllAll′**, with the addition of several nonbonding orbitals that are localized on the indenyl rings. The HOMO is primarily localized on the bridging indenyl ligands, and it is expected that they will be nucleophilic. In contrast, there are noticeable differences between the electronic structures of **CpCp′** and **AllAll′** or **IndInd′**. The two π_{2bCp} orbitals of the Cp ligands form both in-phase and out-of-phase combinations. These orbitals are equivalent to the allyl π_2 orbitals in **AllAll′**, and we have already demonstrated that in **AllAll′** the out-of-phase combination of the π_2 orbitals does not interact with the metal centers. In the case of **CpCp′**, there is a clear bonding interaction between the out-of-phase combination of the two π_{2bCp} orbitals and the metal centers (HOMO-4 in Figure 12). This complements the strong bonding interaction between the in-phase combination of the two π_{2bCp} orbitals and the metal centers (HOMO-12). We believe that the different shape of the π_{2bCp} orbital of Cp in comparison with the π_2 orbital of the allyl ligand and the lack of delocalization in comparison to the $\pi_{2bln(2)}$ orbital of the indenyl ligand allows overlap between the metal 4d orbitals and the out-of-phase combinations of the π_{2bCp} orbitals. In terms of reactivity, the stabilization of the out-of-phase combination of the two π_{2bCp} orbitals in **CpCp′** will presumably attenuate the ability of the Cp ligands to act as nucleophiles, and it is possible that different reactivity may be observed in comparison to **AllAll′** and **IndInd′**.

The HOMO-1 and HOMO in **CpCp′** consist primarily of linear combinations of the π_{2aCp} orbitals, but there is some metal−ligand antibonding character in the HOMO. As a result, the HOMO−LUMO gap in **CpCp′** is significantly smaller (2.97 eV) than the gap in either **AllAll′** (3.79 eV) or **IndInd′** (3.18 eV), where the HOMO is essentially ligand centered and metal−ligand nonbonding. Lower down in the orbital manifold, the HOMO-11 shows a clear bonding interaction between the metal 4d orbitals and the in-phase combination of the π_{2aCp} orbitals. This interaction is only possible because of the *anti* configuration of the two Cp ligands and suggests that in this case the bridging Cp ligand donates more than three electrons. As we have previously noted for **AllAll′**, less back-bonding

dx.doi.org/10.1021/om400415c | *Organometallics* 2013, 32, 4223−4238

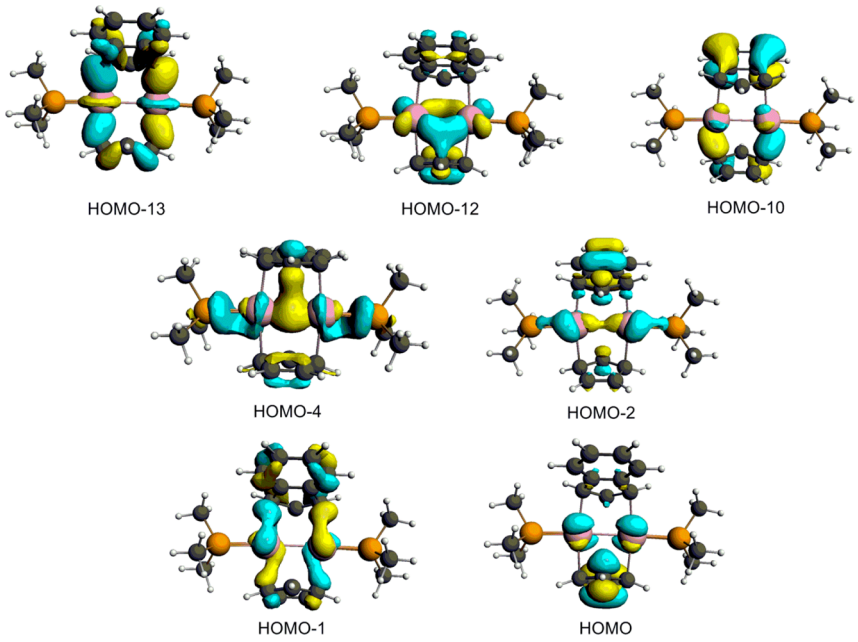

Figure 13. Selected molecular orbitals of **CpInd′**.

occurs in the *anti* configuration in comparison with the *syn* configuration, due to better orbital overlap between the carbon 2p orbitals and the metal centers.[10b] The HOMO-3 clearly shows that back-bonding is not significant in **CpCp′**. Presumably, the decrease in back-bonding is compensated for by the increase in bonding from the π_{2aCp} orbitals, which results in the *anti* geometry being preferred. The bridging allyl ligand has no equivalent to the Cp π_{2aCp} orbitals, and thus bis(allyl) complexes such as **AllAll′** will prefer the *syn* configuration, while we propose that delocalization onto the phenyl ring means that the indenyl π_{2aIn} orbital is not as good a donor as the Cp π_{2aCp} orbital. Therefore, **IndInd′** also prefers the *syn* configuration.

Electronic Structure of the Mixed Cp/Indenyl Complex CpInd′. The complex **CpInd′**, which contains one bridging Cp and one bridging indenyl ligand, has an electronic structure which is most similar to that of the bis(Cp) complex **CpCp′** but also has several features in common with the bis(indenyl) species **IndInd′**. The HOMO contains a weakly antibonding interaction between the Cp π_{2aCp} orbital and the metal 4d orbitals (Figure 13). The corresponding weakly bonding orbital is the HOMO-12, and there is almost no contribution from the indenyl ligand to either the HOMO-12 or HOMO, indicating that this is a highly localized interaction. The antibonding nature of the HOMO means that the HOMO−LUMO gap is small (3.10 eV), which is significantly less than the gap in **AllCp′** (3.57 eV) or **AllInd′** (3.55 eV), which have HOMOs which are primarily nonbonding. The HOMO-1 is the out of phase combination of the Cp π_{2bCp} orbital and the indenyl $\pi_{2bIn(2)}$ orbital, which is partially stabilized by the metal centers, while the out of phase combination of the Cp π_{2bCp} orbital and the indenyl $\pi_{2bIn(1)}$ orbital is the HOMO-10. In this orbital the metal centers only interact with the Cp π_{2bCp} orbital and there is no interaction with the indenyl $\pi_{2bIn(1)}$ orbital, in an analogous fashion to the HOMO-9 in **AllCp′**. The HOMO-13 is the in-phase strongly metal bonding combination of the Cp π_{2bCp} orbital and the indenyl $\pi_{2bIn(1)}$ and $\pi_{2bIn(2)}$ orbitals. As with **IndInd′** and **AllInd′**, the π_{2aIn} orbital of the indenyl ligand is nonbonding and is a large contributor to the HOMO-2, while there is a small amount of back-donation from the metal center to the indenyl ligand (shown in the HOMO-4). There is no back-donation to the Cp ring, suggesting that the indenyl fragment is a better acceptor.

UV−Vis Spectroscopy. Given the differences in the calculated energy of the HOMO−LUMO gaps in the dimers, we performed UV−vis spectroscopy in order to provide verification of our calculations. However, unfortunately the UV−vis spectra of all complexes (see the Supporting Information) were extremely broad in the low-energy region, presumably because there are multiple low-energy transitions. This made pinpointing the energy of the lowest energy transition, which probably corresponds to the HOMO−LUMO gap, difficult. Even when a fitting program was used to model the low-energy absorptions as a series of Gaussian functions, the error in the positions of the peaks remained greater than the differences between the absorptions. However, it is noteworthy that the visual appearance of the compounds supported our hypothesis that the **CpCp** species has the lowest HOMO−LUMO gap, as **CpCp** appeared orange, while all other compounds appeared yellow.

Reactivity with 2,6-Lutidinium Chloride. Our calculations suggest that in all of the complexes studied in this work the bridging ligands are nucleophilic. We have already demonstrated that **AllAll** reacts rapidly with 1 equiv of 2,6-lutidinium chloride to form the complex $(\mu\text{-}C_3H_5)(\mu\text{-Cl})\{Pd(PEt)_3\}_2$, with one bridging allyl ligand and one bridging chloride ligand (Scheme 2).[10a,b,46] Similarly, reaction of **CpCp** with 2,6-lutidinium chloride gives a species with one bridging Cp and one bridging chloride ligand (eq 1).[47] Interestingly, the

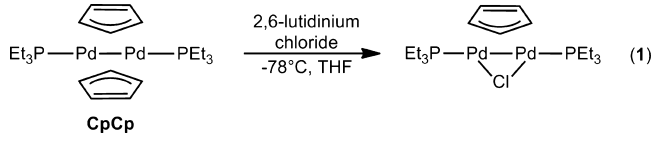

(1)

dx.doi.org/10.1021/om400415c | *Organometallics* 2013, 32, 4223−4238

addition of a second equivalent of 2,6-lutidinium chloride does not lead to further reaction, presumably because in systems with one bridging chloride and one bridging Cp ligand the singly bridging Cp ligand is no longer nucleophilic. We have previously shown that the bridging allyl ligand is not nucleophilic in systems with one bridging allyl and one bridging chloride ligand.[10b] Our results with **CpCp** are consistent with results from Werner and co-workers, who demonstrated that systems containing two bridging Cp ligands react with carboxylic acids and thiols.[5a]

The reactions of the mixed complexes **AllCp**, **AllInd**, and **CpInd** with 2,6-lutidinium chloride are more interesting, as there are issues associated with selectivity. In the cases of **AllCp** and **CpInd**, the **Cp** ligand is selectively protonated to give the complexes $(\mu\text{-}C_3H_5)(\mu\text{-Cl})\{Pd(PEt)_3\}_2$ and $(\mu\text{-indenyl})(\mu\text{-Cl})\{Pd(PEt)_3\}_2$, respectively (eqs 2 and 3). This is consistent with our calculations, which indicate that, in the model complexes **AllCp′** and **CpInd′**, the HOMO is located primarily on the bridging Cp ligand with some metal character. Our results are also in agreement with Werner's observation that weak electrophiles selectively react with the bridging Cp ligand in complexes with one bridging allyl and one bridging Cp ligand.[5a] At this stage it is unclear if protonation occurs directly at the bridging ligand or initially at the metal, followed by reductive elimination of the organic fragment. In contrast, protonation of **AllInd** gives a mixture of $(\mu\text{-}C_3H_5)(\mu\text{-Cl})\{Pd(PEt)_3\}_2$ and $(\mu\text{-indenyl})(\mu\text{-Cl})\{Pd(PEt)_3\}_2$ in a ratio of 7:3, as determined by ^{31}P NMR spectroscopy (eq 4). For the model complex **AllInd′**, the calculations suggest that there is significant character from both the bridging allyl (32%) and the bridging indenyl (68%) in the HOMO, which is consistent with our experimental result of nonselective protonation. Overall, it appears that the nature of the HOMO is a good predictor for the site of protonation in these systems.

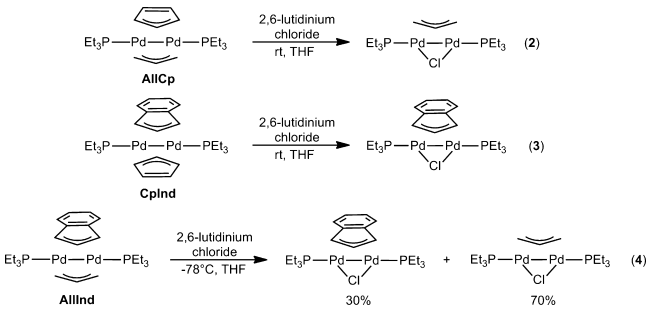

CONCLUSIONS

We have prepared a family of Pd(I) dimers containing bridging allyl, Cp, and indenyl ligands supported by ancillary triethylphosphine ligands. On the basis of both previous experimental results[5a,10a,b,38] and this work we believe that the following conclusions can be made about the structure, bonding, and properties of Pd(I) dimers containing bridging allyl, Cp or indenyl ligands. (i) The primary bonding interaction between the Pd centers and the bridging allyl, Cp, or indenyl ligands occurs through the in-phase combination of the closely related allyl π_2 orbitals, the Cp π_{2bCp} orbitals, and a mixture of the indenyl $\pi_{2bIn(1)}$ and $\pi_{2bIn(2)}$ orbitals. In all cases only three carbon atoms of the bridging ligand interact with the Pd centers. (ii) Bridging Cp and indenyl ligands have Pd−C distances which are consistent with an η^3-Cp or η^3-indenyl ligand in monomeric systems but have fold angles which are consistent with an η^5-Cp or η^5-indenyl ligand in monomeric systems. As a result we suggest that, even though bridging Cp and indenyl ligands only bind through three carbon atoms, they should be classified separately from η^3-Cp or η^3-indenyl ligands. (iii) The bridging fragments bind with different strengths to the Pd_2 core, with allyl binding the tightest and Cp the weakest. (iv) The relative energy of the out-of-phase combination of the allyl π_2 orbitals, the Cp π_{2bCp} orbitals, and the indenyl $\pi_{2bIn(2)}$ orbitals varies depending on whether there is any interaction between the metal centers and these orbitals. Interaction with the metal is more likely for complexes which contain a bridging Cp ligand, and as a result, complexes with a bridging Cp ligand are proposed to be less nucleophilic than those containing bridging allyl or indenyl ligands, where the HOMO is centered on unstabilized ligand orbitals. (v) Bridging allyl and indenyl ligands bind to the metal center as pure three-electron (LX type) ligands, but in the case of Cp there is some additional donation from the π_{2aCp} orbital. As a result the bridging Cp ligand donates more than three electrons. (vi) Cp ligands are more likely to promote an *anti* configuration of the bridging ligands than either allyl or indenyl ligands. (vii) There is back-bonding from the metal to the bridging allyl, Cp, or indenyl ligand in all cases. (vii) There are predictable differences in the ^1H, ^{13}C, and ^{31}P NMR chemical shifts of these complexes, depending on the *trans* influence of the bridging ligand opposite. (viii) The more weakly bound fragment as determined by X-ray crystallography was shown to be the site of reactivity with an electrophile. This was supported by calculations, which indicate that the HOMO is generally localized on the most weakly bound bridging ligand. In future work, we will attempt to use these differences in electronic structure to facilitate different reactivities between the systems.

EXPERIMENTAL SECTION

General Methods. Experiments were performed under a dinitrogen atmosphere in an M. Braun drybox or using standard Schlenk techniques. (Under standard glovebox conditions purging was not performed between uses of pentane, diethyl ether, benzene and toluene; thus, when any of these solvents were used, traces of all these solvents were in the atmosphere and could be found intermixed in the solvent bottles.) Moisture- and air-sensitive liquids were transferred by stainless steel cannula on a Schlenk line or in a drybox. The solvents for air- and moisture-sensitive reactions were dried by passage through a column of activated alumina followed by storage under dinitrogen. All commercial chemicals were used as received except where noted. Triethylphosphine was purchased from Strem Chemicals, NaCp was obtained as a 2 M solution in THF from Acros Organics, and K-Selectride was purchased as 1 M solution in THF from Sigma-Aldrich. CD_2Cl_2, C_6D_6, and d_8-toluene were obtained from Cambridge Isotope Laboratories. CD_2Cl_2 was dried over CaH, while C_6D_6 and d_8-toluene were dried over sodium metal prior to use. NMR spectra were recorded on a Bruker AMX-400 or AMX-500 MHz spectrometer at ambient probe temperatures unless noted. Chemical shifts are reported with respect to residual internal protio solvent for ^1H and $^{13}C\{^1H\}$ NMR spectra and to an external standard for $^{31}P\{^1H\}$ NMR spectra (85% H_3PO_4 in H_2O at δ 0.0 ppm). Robertson Microlit Laboratories, Inc. performed the elemental analyses (inert atmosphere). The following compounds were prepared according to literature procedures: $(\mu\text{-Cl})_2\{Pd(\eta^3\text{-allyl})\}_2$ ($\mathbf{I_{All2}}$),[21] $(\eta^3\text{-allyl})(\eta^5\text{-Cp})Pd$ ($\mathbf{II_{AllInd}}$),[48] 2,6-lutidinium chloride,[49] lithium indenyl,[50] trimethylsilylindene,[51] $(\mu\text{-Cl})_2\{Pd(\eta^3\text{-indenyl})\}_2$ ($\mathbf{I_{Ind2}}$),[22] and **AllAll**.[10a] **CpCp** was synthesized using a modified literature procedure which utilized NaCp instead of TlCp (vide infra).[15c]

X-ray Crystallography. Low-temperature diffraction data (ω scans) were collected on a Rigaku SCXmini diffractometer coupled to a Mercury275R CCD detector with Mo Kα radiation (λ = 0.71073 Å)

dx.doi.org/10.1021/om400415c | *Organometallics* 2013, 32, 4223−4238

for the structures of **AllCp** and **AllInd** and on a Rigaku R-AXIS RAPID diffractometer coupled to a R-AXIS RAPID imaging plate detector with Mo Kα radiation (λ = 0.71073 Å) for the structures of **CpInd** and **CpCp**. All structures were solved by direct methods using SHELXS[52] and refined against F^2 on all data by full-matrix least squares with SHELXL-97[53] using established refinement techniques.[54] All hydrogen atoms were included in the model at geometrically calculated positions and refined using a riding model. The isotropic displacement parameters of all hydrogen atoms were fixed to 1.2 times the U value of the atoms they are linked to (1.5 times for methyl groups). Details of the crystal and refinement data for **AllCp**, **AllInd**, **CpInd**, and **CpCp** are given in the Supporting Information.

Computational Details. All geometry optimizations were performed using Gaussian 09 Revision A.02.[55] After initial optimization of the geometry of **AllAll^{PMe3}**, the TPSSH functional was used in all calculations. The LANL2DZ basis set was used for Pd, and the 6-31G++(d,p) basis set was used for all other atoms. The LANL2DZ pseudopotential was used for Pd. Frequency calculations were performed on all optimized structures to ensure that they were true minima. Fragment analysis was performed using the Amsterdam density functional (version ADF2010.02) package,[56] with the geometry determined from the Gaussian optimization. TZ2P basis sets were used with triple-ξ accuracy sets of Slater-type orbitals, with polarization functions added to all atoms. Relativistic corrections were made using the ZORA (zero-order relativistic approximation) formalism. The TPSSH functional was used to model exchange, as for the Gaussian calculations. The fragment analyses used the molecular orbitals of the chosen fragments as the basis set for the molecular calculations, and initial calculations were carried out on the fragments with the geometry that they had in the molecule. Neutral fragments were chosen, as this assisted in drawing the molecular orbital diagrams. Isosurfaces were drawn using ADFview as implemented in ADF2010.02.

Synthetic Procedures and Characterization Data for New Compounds. ***AllCp***. Triethylphosphine (360 μL, 2.44 mmol) was added to a stirred solution of (η^3-allyl)(η^5-Cp)Pd (520 mg, 2.44 mmol) in toluene (8 mL) at room temperature. An immediate color change from dark red to yellow occurred, and the reaction mixture was stirred for 30 min. The mixture was filtered to remove Pd black, and the solvent was removed under reduced pressure. The yellow solid was then dissolved in pentane. When the mixture stood in a freezer at −35 °C, bright yellow flakes precipitated. **AllCp** was isolated as a yellow powder by decanting the pentane and then removing the residual solvent under reduced pressure (yield 518.4 mg, 76%). Yellow single crystals suitable for X-ray analysis were grown from a saturated pentane solution at −35 °C. Elemental analysis was not performed on this compound due to its thermal instability. NMR spectra are provided in the Supporting Information.

^{1}H NMR (C_6D_6, 500 MHz): δ 6.05 (5H, t, J = 2.1 Hz, *Cp*), 3.00 (1H, m, *central*-allyl), 2.72 (2H, dd, J = 13.1, 6.6 Hz, *syn*-allyl), 1.62 (12H, m, PCH_2CH$_3$), 1.01 (2H, d, J = 12.4 Hz, *anti*-allyl), 0.80 (18H, p, J = 7.6 Hz, PCH$_2$CH_3). ^{31}P{^{1}H} NMR (C_6D_6, 202 MHz): δ 9.09. ^{13}C{^{1}H} NMR (d_8-toluene, 126 MHz): δ 137.4, 88.24, 74.32, 25.59, 17.88 (t, J = 8.9 Hz), 8.42.

(μ-All)(μ-Cl){Pd(PEt$_3$)}$_2$. **AllCp** (50.0 mg, 0.09 mmol) was dissolved in Et$_2$O (5 mL), and 2,6-lutidinium chloride (12.9 mg, 0.09 mmol) was added. The solution was stirred for 1 h at room temperature, and then the solvent was removed under reduced pressure to give **(μ-All)(μ-Cl){Pd(PEt$_3$)}$_2$** as a yellow powder (yield 41.6 mg, 88%). The ^{1}H NMR data were consistent with those previously reported.[10a]

AllInd. Lithium indenyl (34.8 mg, 0.285 mmol) was added to a stirred solution of **(μ-All)(μ-Cl){Pd(PEt$_3$)}$_2$** (150 mg, 0.285 mmol) in toluene (8 mL) at room temperature. An immediate color change from dark red to yellow occurred, and the reaction mixture was stirred for 30 min. The mixture was filtered to remove Pd black, and the solvent was removed from the filtrate under reduced pressure. The yellow solid was then dissolved in pentane. When the mixture stood in a freezer at −35 °C, bright yellow flakes precipitated. **AllInd** was isolated as a yellow powder by decanting the pentane and then removing the residual solvent under reduced pressure (yield 118 mg, 68%) Yellow single crystals suitable for X-ray analysis were grown from a saturated pentane solution at −35 °C. Elemental analysis was not performed on this compound due to its thermal instability. NMR spectra are provided in the Supporting Information.

^{1}H NMR (300 MHz, C_6D_6): δ 7.75 (dd, J = 5.6, 3.2 Hz, 2H, *aromatic*-indenyl), 7.22 (dd, J = 5.7, 3.1 Hz, 2H, *aromatic*-indenyl), 6.03 (dd, J = 6.0 Hz, 2H, *terminal*-indenyl), 4.76 (m, 1H, *central*-indenyl), 3.17 (m, 1H, *central*-allyl), 2.79 (br, 2H, *syn*-allyl), 1.74 (br, 12H, PCH_2CH$_3$), 1.10 (d, J = 12.2 Hz, 2H, *anti*-allyl), 0.69 (p, J = 7.6 Hz, 18H, PCH$_2$CH_3). ^{31}P{^{1}H} NMR (C_6D_6, 121 MHz): δ 10.77. ^{13}C{^{1}H} NMR (C_6D_6, 75 MHz): δ 142.01, 128.59, 120.15, 91.37, 78.67, 49.08, 28.30, 17.54 (t, J = 9.6 Hz), 8.40.

(η^3-Indenyl)PdCl(PEt$_3$). Triethylphosphine (303 μL, 2.06 mmol) in an Et$_2$O solution (5 mL) was added dropwise to a suspension of (μ-Cl)$_2${Pd(η^3-indenyl)}$_2$ (**I$_{Ind2}$**; 528.8 mg, 1.03 mmol) in Et$_2$O (30 mL). There was an immediate lightening of the solution, which upon stirring for 45 min turned red. The solution was filtered to remove Pd black and then concentrated to approximately 12 mL. Pentane (25 mL) was added, and an orange solid precipitated from solution. The solid was isolated by filtration to give **(η^5-Indenyl)PdCl(PEt$_3$)** as an orange powder (yield 619 mg, 80%). Further recrystallization from Et$_2$O layered with pentane yielded an orange powder suitable for elemental analysis.

^{1}H NMR (300 MHz, C_6D_6): δ 7.08 (d, J = 7.4 Hz, 1H, *aromatic*-indenyl), 6.91 (d, J = 7.4 Hz, 1H, *aromatic*-indenyl), 6.82 (t, J = 7.4 Hz, 1H, *aromatic*-indenyl), 6.73 (d, J = 7.4, 1H), 6.19−6.30 (br m, 2H, *terminal*-indenyl), 4.46 (br s, 1 H, *central*-indenyl) 1.35 (dq, J = 10.4 Hz, J = 7.6 Hz, 6H, PCH_2CH$_3$), 0.67 (dt, J = 17.2 Hz, J = 7.6 Hz, 9H, PCH$_2$CH_3). ^{31}P{^{1}H} NMR (CD_2Cl_2, 202 MHz): δ 30.90. ^{13}C{^{1}H} NMR (CD_2Cl_2, 75 MHz): δ 136.97, 135.60, 126.51, 125.64, 119.21, 117.37, 111.10 (d, J = 5.3 Hz), 96.31 (d, J = 22.3 Hz), 70.08 (d, J = 2.8 Hz), 18.09 (d, J = 26.3 Hz) 8.42. Anal. Found (calcd) for $C_{15}H_{22}$ClPPd: C, 47.52 (48.02); H, 5.73 (5.92).

CpInd. *Method A.* To a 20 mL THF solution of **(η^5-Indenyl)PdCl(PEt$_3$)** (120 mg, 0.320 mmol) was added a 2 M THF solution of NaCp (160 μL, 0.320 mmol) at room temperature with stirring. The solution was then heated overnight at 40 °C. The reaction mixture was separated by filtration, and the solvent was removed from the filtrate under reduced pressure. The resultant yellow solid was dissolved in a minimum amount of pentane and allowed to stand overnight at −35 °C. Yellow crystalline solid precipitated from the reaction mixture. The solvent was decanted and the residual solvent removed under reduced pressure to give **CpInd** as a yellow powder (yield 40 mg, 38%).

Method B. A 1 M THF solution of K-Selectride (53 μL, 0.053 mmol) was added dropwise with stirring at −78 °C to a 15 mL THF solution of **(η^3-Indenyl)PdCl(PEt$_3$)** (40 mg, 0.107 mmol). The reaction mixture was warmed to room temperature, and the solution darkened from orange to brown. Stirring was continued for 1 h at room temperature, and then a 2 M THF solution of NaCp (27 μL, 0.053 mmol) was added dropwise to the solution. The reaction mixture was stirred for 2 h, and the mixture was filtered. The solvent was removed from the filtrate under reduced pressure, and the resulting solid was dissolved in a minimum amount of pentane and allowed to stand overnight at −35 °C. Yellow crystalline **CpInd** precipitated as a powder, which was isolated by decanting the pentane and then removing the residual solvent under reduced pressure (yield 8 mg, 54%). Yellow single crystals suitable for X-ray analysis were grown from a saturated pentane solution at −35 °C. Elemental analysis was not performed on this compound due to its thermal instability. NMR spectra are provided in the Supporting Information.

^{1}H NMR (300 MHz, C_6D_6): δ 7.38 (dd, J = 5.6, 3.1 Hz, 2H, *aromatic*-indenyl), 7.02 (dd, J = 5.7, 3.1 Hz, 2H, *aromatic*-indenyl), 5.74 (td, J = 8.3, 3.7 Hz, 2H, *terminal*-indenyl), 3.92 (p, J = 3.1 Hz, 1H, *central*-indenyl), 1.76 (m, 12H, PCH_2CH$_3$), 0.82 (p, J = 7.6 Hz, 18H, PCH$_2$CH_3). ^{31}P{^{1}H} NMR (C_6D_6, 121 MHz): δ 5.22. ^{13}C{^{1}H} NMR (126 MHz, C_6D_6): δ 144.17, 121.67, 120.78, 88.04, 85.24, 47.78, 17.90 (t, J = 8.8 Hz), 8.52.

During the synthesis of **CpInd** using method A, the monomeric complex **(η^1-Cp)(η^3-Indenyl)Pd(PEt$_3$)** was observed as an inter-

mediate by ^{1}H and ^{31}P NMR spectroscopy. NMR data for the intermediate are given below.

^{1}H NMR (300 MHz, C_6D_6): δ 7.66 (dd, J = 15.5, 6.0 Hz, 2H, *aromatic*-indenyl), 7.26 (t, J = 7.1 Hz, 2H, *aromatic*-indenyl), 6.91 (m, 1H, indenyl), 6.79 (d, J = 4.8 Hz, 1H, indenyl), 5.25 (s, 5H, Cp), 4.55 (d, J = 5.4 Hz, 1H, indenyl), 0.95 (m, 6H, PCH_2CH_3), 0.70 (m, 9H, PCH_2CH_3). ^{31}P{^{1}H} NMR (C_6D_6, 202 MHz): δ 30.54.

***CpCp*.** **CpCp** was synthesized using a modified literature procedure which utilized NaCp instead of TlCp.[15c] Initially, $(\mu\text{-Cl}_2)\{Pd(PEt_3)Cl\}_2$ was synthesized using a procedure that was adapted from that described by Duczmal et al. by use of triethylphosphine as the added phosphine and $PdCl_2(PhCN)_2$ rather than $PdCl_2(MeCN)_2$ as the Pd source.[57] The NMR spectroscopic data (^{31}P and ^{1}H) of $(\mu\text{-Cl}_2)\{Pd(PEt_3)Cl\}_2$ were identical with those reported by Heveldt et al.[58] and Grim et al.[59] Subsequently, $(\mu\text{-OAc}_2)\{Pd(PEt_3)Cl\}_2$ was prepared using a procedure that was adapted from Powell et al.[60] by using $(\mu\text{-Cl}_2)\{Pd(PEt_3)Cl\}_2$ as the Pd starting material. Finally, $(\mu\text{-OAc}_2)\{Pd(PEt_3)Cl\}_2$ was converted into **CpCp** using the procedure described by Werner et al.; however, NaCp was used instead of TlCp.[15c]

Representative Procedure for Protonation Reactions. The desired Pd(I) dimer (10 mg) was dissolved in THF (0.25 mL). A suspension of 1 equiv of 2,6-lutidinium chloride in THF (0.25 mL) was added dropwise in the glovebox. The resulting suspension was sonicated for 30 min. In the case of **AllInd** and **CpCp** it was necessary to cool both solutions to −78 °C and warm the NMR tube slowly to room temperature to minimize the formation of side products. The product formed, $(\mu\text{-All})(\mu\text{-Cl})\{Pd(PEt_3)\}_2$,[10a] $(\mu\text{-Cp})(\mu\text{-Cl})\{Pd(PEt_3)\}_2$,[47] or $(\mu\text{-Indenyl})(\mu\text{-Cl})\{Pd(PEt_3)\}_2$, was identified by comparison of the ^{31}P NMR spectra to those of authentic samples.

■ ASSOCIATED CONTENT

Supporting Information

Text, figures, tables, and CIF files giving X-ray information for **AllCp**, **AllInd**, **CpInd**, and **CpCp**, NMR spectra of selected compounds, UV−vis data of selected compounds, details of the choice of functional for DFT calculations, comparison of calculated and experimental structures, more information about fragment calculations, and Cartesian coordinates and energies for optimized structures. This material is available free of charge via the Internet at http://pubs.acs.org.

■ AUTHOR INFORMATION

Corresponding Author

*E-mail for N.H.: nilay.hazari@yale.edu.

Notes

The authors declare no competing financial interest.

■ ACKNOWLEDGMENTS

We gratefully acknowledge support through a Doctoral New Investigator Grant from the ACS Petroleum Research Fund (51009-DNI3). M.J.C. thanks Yale College for funding as part of the Yale Science Scholars Program, and D.P.H. thanks the NSF for support as an NSF Graduate Research Fellow. This work was supported in part by the facilities and staff of the Yale University Faculty of Arts and Sciences High Performance Computing Center and by the National Science Foundation under Grant No. CNS 08-21132 that partially funded acquisition of the facilities.

■ REFERENCES

(1) (a) Tsuji, J. *Perspectives in Organopalladium Chemistry for the 21st Century*; Elsevier: Amsterdam, 1999. (b) Tsuji, J. *Palladium Reagents and Catalysis: Innovations in Organic Synthesis*; Wiley: Chichester, U.K., 1995. (c) Negishi, E.; de Meijre, A. *Organopalladium Chemistry for Organic Synthesis*; Wiley: New York, 2002; Vol. 2.

(2) (a) Trost, B. M.; van Vranken, D. L. *Chem. Rev.* **1996**, *96*, 395. (b) Tsuji, J.; Mandai, T. *Angew. Chem., Int. Ed.* **1995**, *34*, 2589.

(3) Smutny, E. J. *J. Am. Chem. Soc.* **1967**, *89*, 6793.

(4) Szabó, K. J. *Chem. Eur. J.* **2004**, *10*, 5268.

(5) (a) Werner, H. *Adv. Organomet. Chem.* **1981**, *19*, 155. (b) Murahashi, T.; Kurosawa, H. *Coord. Chem. Rev.* **2002**, *231*, 207. (c) Kurosawa, H. *J. Organomet. Chem.* **2004**, *689*, 4511. (d) Hazari, N.; Hruszkewycz, D. P.; Wu, J. *Synlett* **2011**, 1793.

(6) (a) Tromp, M.; Sietsma, J. R. A.; van Bokhoven, J. A.; van Strijdonck, G. P. F.; van Haaren, R. J.; van der Eerden, A. M. J.; van Leeuwen, P. W. N. M.; Koningsberger, D. C. *Chem. Commun.* **2003**, 128. (b) Markert, C.; Neuburger, M.; Kulicke, K.; Meuwly, M.; Pfaltz, A. *Angew. Chem., Int. Ed.* **2007**, *46*, 5892. (c) Paton, R. S.; Brown, J. M. *Angew. Chem., Int. Ed.* **2012**, *51*, 10448.

(7) Weissman, H.; Shimon, L. J. W.; Milstein, D. *Organometallics* **2004**, *23*, 3931.

(8) Elliott, E. L.; Ray, C. R.; Kraft, S.; Atkins, J. R.; Moore, J. S. *J. Org. Chem.* **2006**, *71*, 5282.

(9) Hill, L. L.; Crowell, J. L.; Tutwiler, S. L.; Massie, N. L.; Hines, C. C.; Griffin, S. T.; Rogers, R. D.; Shaughnessy, K. H.; Grasa, G. A.; Johansson Seechurn, C. C. C.; Li, H.; Colacot, T. J.; Chou, J.; Woltermann, C. J. *J. Org. Chem.* **2010**, *75*, 6477.

(10) (a) Hruszkewycz, D. P.; Wu, J.; Hazari, N.; Incarvito, C. D. *J. Am. Chem. Soc.* **2011**, *133*, 3280. (b) Hruszkewycz, D. P.; Wu, J.; Green, J. C.; Hazari, N.; Schmeier, T. J. *Organometallics* **2012**, *31*, 470. (c) Dau, P. D.; Hruszkewcyz, D. P.; Huang, D.-L.; Chalkley, M. J.; Liu, H.-T.; Green, J. C.; Hazari, N.; Wang, L. S. *Organometallics* **2012**, *31*, 8571.

(11) Crabtree, R. H. *The Organometallic Chemistry of the Transition Metals*, 5th ed.; Wiley: New York, 2009.

(12) (a) Werner, H.; Kühn, A. *Angew. Chem., Int. Ed.* **1977**, *16*, 412. (b) Felkin, H.; Turner, G. K. *J. Organomet. Chem.* **1977**, *129*, 429. (c) Jolly, P. W.; Krueger, C.; Schick, K. P.; Wilke, G. *Z. Naturforsch., B: Anorg. Chem., Org. Chem.* **1980**, *35B*, 926. (d) Benn, R.; Jolly, P. W.; Mynott, R.; Raspel, B.; Schenker, G.; Schick, K. P.; Schroth, G. *Organometallics* **1985**, *4*, 1945. (e) Hayashi, Y.; Nakamura, Y.; Isobe, K. *J. Chem. Soc., Chem. Commun.* **1988**, 403. (f) Hayashi, Y.; Matsumoto, K.; Nakamura, Y.; Isobe, K. *J. Chem. Soc., Dalton Trans.* **1989**, 1519. (g) Krause, J.; Cestaric, G.; Haack, K.-J.; Seevogel, K.; Storm, W.; Pörschke, K.-R. *J. Am. Chem. Soc.* **1999**, *121*, 9807. (h) Krause, J.; Goddard, R.; Mynott, R.; Pörschke, K.-R. *Organometallics* **2001**, *20*, 1992.

(13) In this paper the abbreviation **AllAll** means that a complex contains two bridging allyl ligands. The abbreviation Cp is used for a bridging cyclopentadienyl ligand, and Ind is used for a bridging indenyl ligand. Therefore, the abbreviation **CpInd** means that a complex contains one bridging cyclopentadienyl ligand and one bridging indenyl ligand.

(14) (a) Yamamoto, T.; Saito, O.; Yamamoto, A. *J. Am. Chem. Soc.* **1981**, *103*, 5600. (b) Werner, H.; Tune, D.; Parker, G.; Krüger, C.; Brauer, D. J. *Angew. Chem., Int. Ed.* **1975**, *14*, 185. (c) Werner, H.; Kühn, A.; Tune, D. J.; Krueger, C.; Brauer, D. J.; Sekutowski, J. C.; Tsay, Y.-H. *Chem. Ber.* **1977**, *110*, 1763. (d) Kühn, A.; Werner, H. *J. Organomet. Chem.* **1979**, *179*, 421. (e) Norton, D. M.; Mitchell, E. A.; Botros, N. R.; Jessop, P. G.; Baird, M. C. *J. Org. Chem.* **2009**, *74*, 6674.

(15) (a) Werner, H.; Kraus, H.-J. *Angew. Chem., Int. Ed.* **1979**, *18*, 948. (b) Werner, H.; Kraus, H.-J. *J. Chem. Soc., Chem. Commun.* **1979**, 814. (c) Werner, H.; Kraus, H.-J.; Schubert, U.; Ackermann, K. *Chem. Ber.* **1982**, *115*, 2905.

(16) (a) Tanase, T.; Nomura, T.; Yamamoto, Y.; Kobayashi, K. *J. Organomet. Chem.* **1991**, *410*, C25. (b) Tanase, T.; Nomura, T.; Fukushima, T.; Yamamoto, Y.; Kobayashi, K. *Inorg. Chem.* **1993**, *32*, 4578.

(17) It has also been proposed that Pd(I) dimers with bridging benzene ligands and anionic supporting ligands are related to Pd(I) dimers with bridging allyl, Cp, and indenyl ligands and neutral supporting ligands. For examples see: (a) Allegra, G.; Immirzi, A.; Porri, L. *J. Am. Chem. Soc.* **1965**, *87*, 1394. (b) Allegra, G.; Tettamanti Casagrande, G.; Immirzi, A.; Porri, L.; Vitulli, G. *J. Am. Chem. Soc.*

1970, *92*, 289. However, these complexes will not be discussed in this work.
(18) (a) Werner, H. *Adv. Organomet. Chem.* **1981**, *19*, 155. The bonding theory part of this review was taken from unpublished work by P. Hofmann, R. Hoffmann, and P. Dobosh (private communication by these authors to H. Werner). (b) More recent DFT calculations on hypothetical Pd(I) complexes with bridging Cp ligands are also consistent with the Cp ligand acting as a three-electron donor; see: Peng, A.; Zhang, X.; Li, Q.-s.; King, R. B.; Schaefer, H. F., III *New J. Chem.* **2013**, *37*, 775.
(19) (a) Werner, H.; Kühn, A. *J. Organomet. Chem.* **1979**, *179*, 439. (b) Werner, H.; Kraus, H.-J.; Thometzek, P. *Chem. Ber.* **1982**, *1115*, 2914.
(20) From this point forward it should be assumed that the supporting ligand on all complexes is triethylphosphine unless otherwise noted. For example the abbrevation **AllAll** means $(\mu\text{-All})_2\{Pd(PEt_3)\}_2$ and the abbreviation **CpInd** means $(\mu\text{-Cp})(\mu\text{-Ind})\{Pd(PEt_3)\}_2$.
(21) Goliaszewski, A.; Schwartz, J. *Tetrahedron* **1985**, *41*, 5779.
(22) Lin, S.; Boudjouk, P. *J. Chin. Chem. Soc.* **1989**, *36*, 35.
(23) Nakasuji, K.; Yamaguchi, M.; Murata, I.; Tatsumi, K.; Nakamura, A. *Organometallics* **1984**, *3*, 1257.
(24) (a) Sui-Seng, C.; Enright, G. D.; Zargarian, D. *Organometallics* **2004**, *23*, 1236. (b) Hintermann, L.; Lang, F.; Maire, P.; Togni, A. *Eur. J. Inorg. Chem.* **2006**, 1397.
(25) Tatsuno, Y.; Yoshida, T.; Otsuka, S.; Al-Salem, N.; Shaw, B. L. In *Inorganic Syntheses*; Wiley: New York, 1990; p 342.
(26) Ihara, E.; Maeno, Y.; Yasuda, H. *Macromol. Chem. Phys.* **2001**, *202*, 1518.
(27) (a) Henc, B.; Jolly, P. W.; Salz, R.; Stobbe, S.; Wilke, G.; Benn, R.; Mynott, R.; Seevogel, K.; Goddard, R.; Krüger, C. *J. Organomet. Chem.* **1980**, *191*, 449. (b) Krause, J.; Bonrath, W.; Pörschke, K.-R. *Organometallics* **1992**, *11*, 1158.
(28) Werner, H.; Kühn, A. *Angew. Chem., Int. Ed.* **1979**, *18*, 416.
(29) (a) Veiros, L. F. *Organometallics* **2000**, *19*, 5549. (b) Calhorda, M. J.; Felix, V.; Veiros, L. F. *Coord. Chem. Rev.* **2002**, *230*, 49.
(30) Farrugia, L. J. *J. Appl. Crystallogr.* **1997**, *30*, 565.
(31) (a) Faller, J. W.; Crabtree, R. H.; Habib, A. *Organometallics* **1985**, *4*, 929. (b) O'Connor, J. M.; Casey, C. P. *Chem. Rev.* **1987**, *87*, 307. (c) Calhorda, M. J.; Veiros, L. F. *Comments Inorg. Chem.* **2001**, *22*, 375.
(32) For Cp systems the fold angle is defined as the difference in the dihedral angles between the plane defined by the three allylic carbons and that formed by the carbon atoms of Cp except for the central bridging carbon atom, whereas for indenyl systems the fold angle is defined as the difference in the dihedral angles between the plane defined by the three allylic carbons and that formed by the benzenoid carbons.
(33) Vicente, J.; Abad, J.-A.; Bergs, R.; Jones, P. G.; Ramirez de Arellano, M. C. *Organometallics* **1996**, *15*, 1422.
(34) Jose, M.; Veiros, L. F. *Coord. Chem. Rev.* **1999**, *185−186*, 37.
(35) Nakasuji, K.; Yamaguchi, M.; Murata, I.; Tatsumi, K.; Nakamura, A. *Organometallics* **1984**, *3*, 1257.
(36) Tanase, T.; Fukushima, T.; Nomura, T.; Yamamoto, Y.; Kobayashi, K. *Inorg. Chem.* **1994**, *33*, 32.
(37) (a) Budzelaar, P. H. M.; Boersma, J.; Van der Kerk, G. J. M.; Spek, A. L. *Organometallics* **1984**, *3*, 1187. (b) Beck, R.; Johnson, S. A. *Organometallics* **2013**, *32*, 2944. (c) Heinemann, O.; Jolly, P. W.; Krüger, C.; Verhovnik, G. P. J. *Organometallics* **1996**, *15*, 5462. (d) Sieb, D.; Schuhen, K.; Morgen, M.; Herrmann, H.; Wadepohl, H.; Lucas, N. T.; Baker, R. W.; Enders, M. *Organometallics* **2012**, *31*, 356.
(38) Kurosawa, H.; Hirako, K.; Natsume, S.; Ogoshi, S.; Kanehisa, N.; Kai, Y.; Sakaki, S.; Takeuchi, K. *Organometallics* **1996**, *15*, 2089.
(39) Veiros, L. F. *Organometallics* **2000**, *19*, 3127.
(40) (a) Sergeyev, N. M. *Prog. Nucl. Magn. Reson. Spectrosc.* **1975**, *9*, 71. (b) Köhler, F. H. *Chem. Ber.* **1974**, *574*, 570. (c) Zargarian, D. *Coord. Chem. Rev.* **2002**, *233−234*, 157.
(41) (a) Lehmkuhl, H.; Näser, J.; Mehler, G.; Keil, T.; Danowski, F.; Benn, R.; Mynott, R.; Schroth, G.; Gabor, B.; Krüger, C.; Betz, P. *Chem. Ber.* **1991**, *124*, 441. (b) Lehmkuhl, H.; Dimitrov, V. J. *Organomet. Chem.* **1996**, *519*, 83. (c) Filipuzzi, S.; Pregosin, P. S.; Albinati, A.; Rizzato, S. *Organometallics* **2008**, *27*, 437.
(42) (a) Merola, J. S.; Kacmarcik, R. T.; Van Engen, D. *J. Am. Chem. Soc.* **1986**, *108*, 329. (b) Fessenbecker, A.; Stephan, M.; Grimes, R. N.; Pritzkow, H.; Zenneck, U.; Siebert, W. *J. Am. Chem. Soc.* **1991**, *113*, 3061. (c) Huber, T. A.; Belanger-Gariepy, F.; Zargarian, D. *Organometallics* **1995**, *14*, 4997.
(43) Baker, R. T.; Tulip, T. H. *Organometallics* **1986**, *5*, 839.
(44) (a) Elian, M.; Hoffmann, R. *Inorg. Chem.* **1975**, *14*, 5. (b) Hoffmann, R.; Albright, T. A.; Thorn, D. L. *Pure Appl. Chem.* **1978**, *50*, 1.
(45) Sakaki, S.; Takeuchi, K.; Sugimoto, M.; Kurosawa, H. *Organometallics* **1997**, *16*, 2995.
(46) Hruszkewycz, D. P.; Hazari, N. Unpublished results.
(47) Werner, H.; Thometzek, P.; Krüger, C.; Kraus, H.-J. *Chem. Ber.* **1986**, *119*, 2777.
(48) Tatsuno, Y.; Yoshida, T.; Otsuka, S. *Inorg. Synth.* **1990**, *28*, 342.
(49) (a) Grönberg, K. L. C.; Henderson, R. A.; Oglieve, K. E. *J. Chem. Soc., Dalton Trans.* **1998**, 3093. (b) Garratt, S. A.; Hughes, R. P.; Kovacik, I.; Ward, A. J.; Willemsen, S.; Zhang, D. J. *Am. Chem. Soc.* **2005**, *127*, 15585.
(50) Wang, H.; Wang, H.; Li, H.; Xie, Z. *Organometallics* **2004**, *23*, 875.
(51) Görl, C.; Alt, H. G. *J. Organomet. Chem.* **2007**, *692*, 4580.
(52) Sheldrick, G. M. *Acta Crystallogr., Sect. A* **1990**, *46*, 467.
(53) Sheldrick, G. M. *Acta Crystallogr., Sect. A* **2008**, *64*, 112.
(54) Müller, P. *Crystallogr. Rev.* **2009**, *15*, 57.
(55) Frisch, M. J.; Trucks, G. W.; Schlegel, H. B.; Scuseria, G. E.; Robb, M. A.; Cheeseman, J. R.; Scalmani, G.; Barone, V.; Mennucci, B.; Petersson, G. A.; Nakatsuji, H.; Caricato, M.; Li, X.; Hratchian, H. P.; Izmaylov, A. F.; Bloino, J.; Zheng, G.; Sonnenberg, J. L.; Hada, M.; Ehara, M.; Toyota, K.; Fukuda, R.; Hasegawa, J.; Ishida, M.; Nakajima, T.; Honda, Y.; Kitao, O.; Nakai, H.; Vreven, T.; Montgomery, J. A., Jr.; Peralta, J. E.; Ogliaro, F.; Bearpark, M.; Heyd, J. J.; Brothers, E.; Kudin, K. N.; Staroverov, V. N.; Kobayashi, R.; Normand, J.; Raghavachari, K.; Rendell, A.; Burant, J. C.; Iyengar, S. S.; Tomasi, J.; Cossi, M.; Rega, N.; Millam, N. J.; Klene, M.; Knox, J. E.; Cross, J. B.; Bakken, V.; Adamo, C.; Jaramillo, J.; Gomperts, R.; Stratmann, R. E.; Yazyev, O.; Austin, A. J.; Cammi, R.; Pomelli, C.; Ochterski, J. W.; Martin, R. L.; Morokuma, K.; Zakrzewski, V. G.; Voth, G. A.; Salvador, P.; Dannenberg, J. J.; Dapprich, S.; Daniels, A. D.; Farkas, Ö.; Foresman, J. B.; Ortiz, J. V.; Cioslowski, J.; Fox, D. J. *Gaussian 09, Revision A.02*; Gaussian, Inc., Wallingford, CT, 2009.
(56) (a) te Velde, G.; Bickelhaupt, F. M.; Baerends, E. J.; Fonseca Guerra, C.; Van Gisbergen, S. J. A.; Snijders, J. G.; Ziegler, T. *J. Comput. Chem.* **2001**, *22*, 931. (b) Fonseca Guerra, C.; Snijder, J. G.; te Velde, G.; Baerends, E. J. *Theor. Chem. Acc.* **1998**, *99*, 391. (c) *ADF2010*; SCM, Theoretical Chemistry, Vrije Universiteit, Amsterdam, The Netherlands; http://www.scm.com.
(57) Noskowska, M.; Sliwinska, E.; Duczmal, W. *Transition Met. Chem.* **2003**, *28*, 756.
(58) Fergusson, J. E.; Heveldt, P. F. *Inorg. Chim. Acta* **1978**, *31*, 145.
(59) Grim, S. O.; Keiter, R. L. *Inorg. Chim. Acta* **1970**, *4*, 56.
(60) Powell, J.; Jack, T. *Inorg. Chem.* **1972**, *11*, 1039.